

Sterile neutrinos in leptonic and semileptonic decays

A. Abada^a, A.M. Teixeira^b, A. Vicente^{a,c} and C. Weiland^{d,e}

^a Laboratoire de Physique Théorique, CNRS – UMR 8627,
Université de Paris-Sud 11, F-91405 Orsay Cedex, France

^b Laboratoire de Physique Corpusculaire, CNRS/IN2P3 – UMR 6533,
Campus des Cézeaux, 24 Av. des Landais, F-63171 Aubièrre Cedex, France

^c IFPA, Dep. AGO, Université de Liège,
Bat B5, Sart-Tilman B-4000 Liège 1, Belgium

^d Departamento de Física Teórica, Universidad Autónoma de Madrid,
Cantoblanco, Madrid 28049, Spain

^e Instituto de Física Teórica UAM/CSIC,
Calle Nicolás Cabrera 13-15, Cantoblanco, Madrid 28049, Spain

Abstract

We address the impact of a modified $W\ell\nu$ coupling on a wide range of observables, such as τ leptonic and mesonic decays, leptonic decays of pseudoscalar mesons, as well as semileptonic meson decays. In particular, we concentrate on deviations from lepton flavour universality, focusing on the ratios $R_P = \Gamma(P \rightarrow \ell\nu)/\Gamma(P \rightarrow \ell'\nu)$, with $P = K, \pi, D, D_s$, $R(D) = \Gamma(B^+ \rightarrow D\tau^+\nu)/\Gamma(B^+ \rightarrow D\ell^+\nu)$, $R_\tau = \Gamma(\tau \rightarrow \mu\nu\nu)/\Gamma(\tau \rightarrow e\nu\nu)$, $R_P^{\ell\tau} = \Gamma(\tau \rightarrow P\nu)/\Gamma(P \rightarrow \ell\nu)$, and $\text{BR}(B \rightarrow \tau\nu)$. We further consider leptonic gauge boson decays, such as $W \rightarrow \ell\nu$ and $Z \rightarrow \nu\nu$. For all the above observables, we provide the corresponding complete analytical expressions, derived for the case of massive neutrinos. Working in the framework of the Standard Model extended by additional sterile fermions, which mix with the active (left-handed) neutrinos, we numerically study the impact of active-sterile mixings on the above mentioned observables.

1 Introduction

In order to account for neutrino masses and mixings, the Standard Model (SM) can be extended with new sterile fermionic states, such as right-handed neutrinos. Sterile states are present in several neutrino mass models, and their existence is also strongly motivated by current data from reactor experiments, cosmology, as well as indications from large scale structure formation [1, 2]. In these frameworks, leptonic charged currents can be modified due to the mixings of the sterile

neutrinos with the active left-handed ones. The SM flavour-conserving term in the lepton weak charged current Lagrangian is modified as

$$-\mathcal{L}_{\text{cc}} = \frac{g}{\sqrt{2}} U^{ji} \bar{\ell}_j \gamma^\mu P_L \nu_i W_\mu^- + \text{c.c.}, \quad (1)$$

where U is a generic leptonic mixing matrix, $i = 1, \dots, n_\nu$ denotes the physical neutrino states and $j = 1, \dots, 3$ the flavour of the charged leptons. In the case of three neutrino generations, U corresponds to the unitary PMNS matrix, U_{PMNS} . The mixing between the left-handed leptons, here denoted by \tilde{U}_{PMNS} , now corresponds to a 3×3 block of U , which can be parametrised as

$$U_{\text{PMNS}} \rightarrow \tilde{U}_{\text{PMNS}} = (\mathbb{1} - \eta) U_{\text{PMNS}}, \quad (2)$$

where the matrix η contains the deviation of \tilde{U}_{PMNS} from unitarity [3, 4].

The active-sterile mixings and the departure from unitarity of \tilde{U}_{PMNS} can have an impact on several observables, inducing deviations from SM predictions, such as violation of lepton flavour universality (LFU) [5–7], enhanced lepton flavour violating (LFV) processes [8, 9] and new contributions to different low-energy rare decays.

In this work we address the impact of the modified charged current vertex on several observables, whose dominant SM contribution arises from tree-level W exchange. This is the case of decays with one or two neutrinos in the final state, as for example τ leptonic and mesonic decays, leptonic π , K , D , D_s , B decays and semileptonic meson decays, like $B \rightarrow D \ell \nu$. We also consider leptonic gauge boson decays, such as $W \rightarrow \ell \nu$ and $Z \rightarrow \nu \nu$. Despite the fact that the hadronic sector can also be affected by some underlying New Physics (NP) contributions, in our analysis we decouple these effects, assuming that all NP effects are encoded in the modified leptonic weak current vertices, due to the presence of extra sterile neutrinos. To do so, and for all the observables mentioned above, we derive the corresponding complete analytical expressions in this context, in particular, fully accounting for massive charged and neutral fermions as well as mixing in the lepton sector.

The deviations from unitarity as well as the possibility of having the sterile states as final decay products might induce departures from the SM theoretical expectations. Due to these potential contributions, these frameworks are severely constrained: any realisation must comply with a number of laboratory bounds, electroweak (EW) precision tests and cosmological constraints, among others.

The modified $W \ell \nu$ vertex, and the associated new contributions to the different observables mentioned above can be found in several scenarios with additional singlet states, as is the case of the νSM [10], the low-scale type-I seesaw [11] and the Inverse Seesaw (ISS) [12], among other possibilities. For the purpose of our numerical analysis, it is convenient to consider a specific seesaw realisation which consists of an extension of the SM field content by sterile neutrinos. As done in a first study devoted to LFU violation in kaon and pion leptonic decays [7], we consider here the ISS, which has the appealing feature of naturally having large Yukawa couplings and a comparatively light sterile spectrum at the same time, thus increasing the active-sterile mixing. It is nevertheless worth pointing out that our results are quite general, since they only depend on the modified $W \ell \nu$ vertex. Therefore, and although we choose a specific framework, the qualitative conclusions here derived should in principle hold for other models.

Our work is organised as follows: in Section 2 we address in detail the departure from unitarity of the \tilde{U}_{PMNS} matrix, focusing on the different constraints arising from neutrino data, electroweak observables, laboratory measurements and cosmological observations. In Section 3, we discuss the observables considered, presenting analytical formulae, and we summarise the corresponding SM

expectations and experimental status. The numerical results (for the specific realisation of the ISS considered) are collected and discussed in Section 4, while our concluding remarks are given in Section 5.

2 The SM extended by fermionic gauge singlets

One of the simplest extensions of the SM allowing to accommodate massive neutrinos consists in the introduction of right-handed states ν_R , singlets under the SM gauge group. The SM mass Lagrangian is enlarged with a Dirac mass term $m_D \bar{\nu}_R \nu_L$, and should lepton number violation be allowed, with a Majorana mass term $m_M \bar{\nu}_R^c \nu_R$. Within this class of models, the standard type-I seesaw [13–15] is an appealing framework, where a natural explanation for the smallness of neutrino masses can be found by assuming that the Majorana masses of the right-handed neutrinos are large, leading to a suppression of $m_\nu \sim m_D^2/m_M$.

However, the large mass scales usually involved, typically much larger than the electroweak scale, imply that no direct experimental tests of the standard type-I seesaw model are possible. Low-scale seesaw models, in which the new singlet fermions are lighter, with masses around the electroweak scale, are more attractive from a phenomenological point of view. In this case, the new states can be produced in collider or low-energy experiments and their contributions to physical processes can be sizable. In our work we will consider this type of models¹.

2.1 Impact for charged currents: the $W\ell\nu$ vertex

In the framework of the SM extended to accommodate massive neutrinos, the lepton weak charged current Lagrangian is given by $-g/\sqrt{2} J^\mu W_\mu^- + \text{c.c.}$, where $J^\mu = \bar{\ell} U \gamma^\mu P_L \nu$, with $P_L = (\mathbb{1} - \gamma_5)/2$ and

$$U = V^\dagger U_\nu. \quad (3)$$

In the above, V and U_ν are unitary transformations that relate the physical ℓ and ν states to the gauge eigenstates ℓ' and ν' as

$$\ell' = V \ell, \quad \nu' = U_\nu \nu, \quad (4)$$

and the matrix U is thus the leptonic mixing matrix (the analog of the CKM matrix in the quark sector); just as in the quark sector, where the flavour structure of the CKM matrix leads to a very rich phenomenology, the leptonic mixing matrix also has an impact on many observables related to lepton flavour.

The above discussion is generic, and holds in scenarios with additional singlet neutrinos. However, since only left-handed leptons participate in the charged interaction, in this case U is a rectangular matrix which can be written as

$$U = \left(\tilde{U}_{\text{PMNS}}, U_{AS} \right), \quad (5)$$

where \tilde{U}_{PMNS} is a 3×3 matrix and U_{AS} is a $3 \times (n_\nu - 3)$ matrix, with n_ν the total number of neutrino states. While the rows of U are indeed unit vectors ($U U^\dagger = \mathbb{1}$), the \tilde{U}_{PMNS} and U_{AS} submatrices are not unitary [3].

One can easily interpret the matrices \tilde{U}_{PMNS} and U_{AS} . In the case of three neutrino generations (no additional sterile states), U corresponds to the unitary PMNS matrix and thus one can identify

¹An interesting realisation of low-scale seesaw models is the so-called Inverse Seesaw [12], which will be briefly reviewed in Section 4.1 and subsequently used in the numerical analysis.

$\tilde{U}_{\text{PMNS}} = U_{\text{PMNS}}$. However, in general, the mixing among the left-handed leptons is given by a non-unitary \tilde{U}_{PMNS} , usually parametrised as already introduced in Eq. (2),

$$\tilde{U}_{\text{PMNS}} = (\mathbb{1} - \eta) U_{\text{PMNS}}.$$

Finally, the matrix U_{AS} contains information about the mixing between the active neutrinos and the sterile singlet states.

2.2 Constraints from neutrino data

Any neutrino motivated extension of the SM must accommodate oscillation data [16–18]. In our analysis, we consider both possible (normal and inverted) hierarchies for the light neutrino spectrum and take the current best-fit results on the oscillation parameters as obtained in [16]. For a normal hierarchy this implies the following values

$$\begin{aligned} \sin^2 \theta_{12} &= 0.32, & \sin^2 \theta_{23} &= 0.427, & \sin^2 \theta_{13} &= 0.0246, \\ \Delta m_{21}^2 &= 7.62 \times 10^{-5} \text{eV}^2, & |\Delta m_{31}^2| &= 2.55 \times 10^{-3} \text{eV}^2. \end{aligned} \quad (6)$$

Note that we have taken the local minimum for θ_{23} in the first octant, in agreement with [17]. On the other hand, for an inverted hierarchy we have

$$\begin{aligned} \sin^2 \theta_{12} &= 0.32, & \sin^2 \theta_{23} &= 0.6, & \sin^2 \theta_{13} &= 0.025, \\ \Delta m_{21}^2 &= 7.62 \times 10^{-5} \text{eV}^2, & |\Delta m_{31}^2| &= 2.43 \times 10^{-3} \text{eV}^2. \end{aligned} \quad (7)$$

Although no data on the CP violating phases is available, we have also investigated the effect of the Dirac phase in our analysis.

As recently pointed out [19], a combination of solar neutrino experiments, medium-baseline and short-baseline reactor antineutrino experiments could allow to perform the first direct unitarity test of the PMNS matrix.

Bounds on the non-unitarity matrix η , defined in Eq. (2), were derived using Non-Standard Interactions [20]. However, they were obtained by means of an effective theory approach, and thus their application in our numerical study will be limited to the cases in which the latter approach is valid.

2.3 Constraints from EW precision tests

Let us begin by briefly commenting on the constraints derived from global fits to electroweak precision data. In the presence of singlet neutrinos, electroweak precision constraints were first addressed in [21] and recently studied in [22, 23]. In [21], an effective approach was used, and thus these constraints will only be considered in cases with multi-TeV singlet states. Our numerical results, which will be presented in Section 4, are in agreement with the results of [22, 23].

Z invisible decay width

The comparison of the SM prediction of the Z invisible decay width to the LEP measurement [24],

$$\Gamma_{\text{SM}}(Z \rightarrow \nu\nu) = (501.69 \pm 0.06) \text{MeV}, \quad (8)$$

$$\Gamma_{\text{Exp}}(Z \rightarrow \nu\nu) = (499.0 \pm 1.5) \text{MeV}, \quad (9)$$

suggests that the experimental value is $\sim 2\sigma$ below the theoretical expectation of the SM. In order to investigate if the presence of sterile fermions could have an impact on the decay width $\Gamma(Z \rightarrow \nu\nu)$, one needs to consider the latter decay in the general case of massive Majorana neutrinos. The invisible Z decay width reads

$$\Gamma(Z \rightarrow \nu\nu) = \sum_{i,j} \Delta_{ij} \Gamma_{VFF}(m_Z, m_{\nu_i}, m_{\nu_j}, b_L^{ij}, b_R^{ij}), \quad (10)$$

where $i, j = 1, \dots, N_{\max}$ (N_{\max} corresponding to the heaviest ν which is kinematically allowed). The function $\Gamma_{VFF} \equiv \Gamma_{VFF}(m_V, m_{F_1}, m_{F_2}, b_L, b_R)$ is given by

$$\Gamma_{VFF} = \frac{\lambda^{1/2}(m_V, m_{F_1}, m_{F_2})}{48\pi m_V^3} \times \left[(|b_L|^2 + |b_R|^2) \left(-\frac{(m_{F_1}^2 - m_{F_2}^2)^2}{m_V^2} - m_{F_1}^2 - m_{F_2}^2 + 2m_V^2 \right) + 12m_{F_1}m_{F_2}\text{Re}(b_L b_R^*) \right]. \quad (11)$$

In the above, the kinematical function $\lambda(a, b, c)$ is defined as

$$\lambda(a, b, c) = (a^2 - b^2 - c^2)^2 - 4b^2c^2, \quad (12)$$

and the couplings $b_{L,R}$ are

$$\begin{aligned} b_L^{ij} &= 2^{1/4} m_Z \sqrt{G_F} \sum_{a=1}^3 U_{ai}^* U_{aj}, \\ b_R^{ij} &= -\left(b_L^{ij}\right)^*. \end{aligned} \quad (13)$$

Finally, $\Delta_{ij} = 1 - \frac{1}{2}\delta_{ij}$ is a factor which accounts for the Majorana nature of the neutrinos.

Since the latter expressions depend on the entries of the mixing matrix U , and given that the sum in Eq. (10) involves all neutrino states that are kinematically allowed, the Z invisible decay width is an important constraint that any model involving fermionic gauge singlets should satisfy.

2.4 Other constraints

Sterile neutrinos can be produced in meson decays such as $\pi^\pm \rightarrow \mu^\pm \nu$, with rates dependent on their mixing with the active neutrinos. Negative searches for monochromatic lines in the muon spectrum can be translated into bounds for $m_{N_s} - \theta_{\mu s}$ combinations, where m_{N_s} is the mass of one of the sterile states and $\theta_{\mu s}$ parametrises the active-sterile mixing [1, 25]. All experimental searches performed so far have led to negative results, allowing to set stringent limits for sterile neutrinos with masses in the MeV-GeV range and fuelling plans for future experiments [26].

Unless the active-sterile mixings are negligible, the modified $W\ell\nu$ vertex may also contribute to LFV processes, with rates potentially larger than current bounds. The radiative muon decay $\mu \rightarrow e\gamma$, searched for by the MEG experiment [27], provides the most stringent constraint. The rate induced by sterile neutrinos² should obey [8, 9]

$$\text{BR}(\mu \rightarrow e\gamma) = \frac{\alpha_W^3 s_W^2 m_\mu^5}{256 \pi^2 m_W^4 \Gamma_\mu} |H_{\mu e}|^2 \leq 5.7 \times 10^{-13}, \quad (14)$$

²We have assumed a dipole dominated LFV phenomenology. In this case $\mu \rightarrow e\gamma$ is the most constraining LFV observable. However, it has been recently pointed out that in low-scale seesaw models, the dominant contributions might come from (non-supersymmetric) box diagrams [28–31]. In this case, the expected future sensitivity of $\mu - e$ conversion experiments can also play a relevant rôle in detecting and/or constraining sterile neutrino scenarios. Similarly, supersymmetric models may have dominant contributions beyond the dipole one [32].

where $H_{\mu e} = \sum_i U^{2i} U^{1i*} G_\gamma \left(\frac{m_{\nu, i+3}^2}{m_W^2} \right)$, G_γ being the associated loop function and U the mixing matrix defined in Eq. (1). In addition, α_W and $s_W = \sin \theta_W$ denote the weak coupling and mixing angle, respectively, while Γ_μ corresponds to the total muon width.

At higher energies, constraints on sterile neutrinos can also be derived from Higgs decays. LHC data already provides some important bounds when the sterile states are slightly below 125 GeV, due to the potential Higgs decays to left- and right-handed neutrinos. This has been recently studied in [33–35].

Finally, in the presence of lepton number violating (LNV) interactions, as is the case for singlet neutrinos with Majorana masses, new processes are possible. Although neutrinoless double beta decay [36] remains the key observable (the most recent results on neutrinoless double beta decay having been obtained by the GERDA experiment [37]), the LHC is beginning to be competitive, as demonstrated by the phenomenological studies of [38, 39] and recent CMS results [40]. However, we have not taken these LNV processes into account, since they are not correlated with the observables of interest for our study³.

2.5 Constraints from cosmology

Under the assumption of a standard cosmology, the most constraining bounds on sterile neutrinos with a mass below the TeV arise from a wide variety of cosmological observations [1, 41]. Sterile neutrinos can constitute a non-negligible fraction of the dark matter of the Universe and thus influence structure formation, which is constrained by Large Scale Structure and Lyman- α data. Active-sterile mixing also induces the radiative decays $\nu_i \rightarrow \nu_j \gamma$, well constrained by cosmic X-ray searches. Lyman- α limits, the existence of additional degrees of freedom at the epoch of Big Bang Nucleosynthesis, and Cosmic Microwave Background data (among others), allow to set additional bounds in the $m_{N_s} - \theta_{is}$ plane. However, all the above cosmological bounds can be evaded if a non-standard cosmology is considered, for example in scenarios with a low reheating temperature [42], or when sterile neutrinos couple to a dark sector [43]. In our numerical analysis we will allow for the violation of the latter bounds in some scenarios, explicitly stating it.

3 Observables

We now proceed to derive the new contributions to a number of observables involving the $W \rightarrow \ell \nu$ vertex. Some of these expressions have also been derived in [44]. Although for many of the considered observables there is a good agreement between the SM expectations and experimental measurements, for some others there is a manifest tension between theoretical predictions and experimental results. We will explore how extending the SM by sterile neutrinos might contribute to alleviate some of the latter tensions. This will depend on the sterile neutrino masses and on their mixings with the active neutrinos. Should the sterile fermions be light, they can be kinematically available as final states of a given decay, leading in some cases to a further enhancement from phase space effects. In this work we thus address (when possible) observables which allow to reduce the need of hadronic input.

³As mentioned in Section 2.2, we take vanishing Majorana phases. The latter have no impact on the observables studied in this work but may possibly be used as degrees of freedom to lower the rates for LNV processes below current bounds.

3.1 $W \rightarrow \ell\nu$ decays

We first consider the observable most directly affected by the sterile fermions - W leptonic decays, $\text{BR}(W \rightarrow \ell_i\nu)$. The width of the $W \rightarrow \ell_i\nu$ decay is given by

$$\Gamma(W \rightarrow \ell_i\nu) = \sum_{j=1}^{N_{\max}^{(\ell_i)}} \Gamma_{VFF}(m_W, m_{\ell_i}, m_{\nu_j}, a_L^{ij}, 0), \quad (15)$$

where the functions Γ_{VFF} and $\lambda(m_W, m_{F_1}, m_{F_2})$ are given in Eqs. (11) and (12), respectively. The couplings a_L are defined as

$$a_L^{ij} = 2^{3/4} m_W \sqrt{G_F} U_{ij}. \quad (16)$$

Not necessarily all ν_j can be final products of the decay. We denote by $N_{\max}^{(\ell_i)}$ the N^{th} heaviest neutrino mass eigenstate which is kinematically allowed when the lepton produced is ℓ_i . Notice that the SM result can be easily recovered by taking the limits $m_{\nu_j} = 0$ and $U^{ji} = \delta_{ji}$. Our result translates into corrections to $\text{BR}(W \rightarrow e\nu)$, $\text{BR}(W \rightarrow \mu\nu)$ and $\text{BR}(W \rightarrow \tau\nu)$, whose experimental values [24] and SM predictions⁴ [45] exhibit at present a small tension,

$$\text{BR}(W \rightarrow e\nu)^{\text{SM}} = 0.108383 \quad \text{BR}(W \rightarrow e\nu)^{\text{Exp}} = 0.1080 \pm 0.009 \quad (17)$$

$$\text{BR}(W \rightarrow \mu\nu)^{\text{SM}} = 0.108383 \quad \text{BR}(W \rightarrow \mu\nu)^{\text{Exp}} = 0.1075 \pm 0.0013 \quad (18)$$

$$\text{BR}(W \rightarrow \tau\nu)^{\text{SM}} = 0.108306 \quad \text{BR}(W \rightarrow \tau\nu)^{\text{Exp}} = 0.1057 \pm 0.0015. \quad (19)$$

The tension between LEP-II results [46] and the SM prediction on $W \rightarrow \ell\nu$ decays has not been given a large attention but for a few exceptions, see for example [47].

3.2 τ decays

Due to its comparatively large mass, the tau lepton can have both leptonic and mesonic decays, for example into pions or kaons. Here we discuss how the corrections to the $W\ell\nu$ vertex can affect the W -mediated tree-level τ decays.

Leptonic τ decays

Flavour universality in leptonic τ decays is parametrised by the quantity R_τ ,

$$R_\tau \equiv \frac{\Gamma(\tau^- \rightarrow \mu^- \nu\nu)}{\Gamma(\tau^- \rightarrow e^- \nu\nu)}. \quad (20)$$

In the SM (with vanishing m_ν) one has $R_\tau \simeq 0.973$ [48]. Experimentally, this observable has been measured to a precision better than the individual decay widths by the BaBar [49] and CLEO [50] experiments, with the following values

$$R_\tau = 0.9796 \pm 0.0016 \pm 0.0036 \text{ (BaBar)}, \quad R_\tau = 0.9777 \pm 0.0063 \pm 0.0087 \text{ (CLEO)}, \quad (21)$$

while the current global fit stands at $R_\tau = 0.9764 \pm 0.0030$ [24].

⁴Here we quote the 1-loop calculation of [45], where $m_H \sim 100$ GeV was used.

In the presence of additional sterile fermions, the decay width $\Gamma(\ell_i \rightarrow \ell_j \nu \nu)$ must be corrected⁵ and after summing over all the kinematically accessible neutrinos, one finds, under the assumption of a Majorana nature for the neutrinos,

$$\Gamma_{\text{tot}} = \sum_{\alpha=1}^{N_{\text{max}}^{(\ell_j)}} \sum_{\beta=1}^{\alpha} \Gamma_{\alpha\beta}, \quad (22)$$

with

$$\begin{aligned} \Gamma_{\alpha\beta} = & \frac{G_F^2 (2 - \delta_{\alpha\beta})}{m_{\ell_i}^3 (2\pi)^3} \int_{(m_{\ell_j} + m_{\nu_\alpha})^2}^{(m_{\ell_i} - m_{\nu_\beta})^2} ds_{j\alpha} \left[\frac{1}{4} |U_{i\alpha}|^2 |U_{j\beta}|^2 (s_{j\alpha} - m_{\ell_j}^2 - m_{\nu_\alpha}^2) (m_{\ell_i}^2 + m_{\nu_\beta}^2 - s_{j\alpha}) \right. \\ & \left. + \frac{1}{2} \Re(U_{i\alpha}^* U_{j\beta} U_{i\beta} U_{j\alpha}^*) m_{\nu_\alpha} m_{\nu_\beta} \left(s_{j\alpha} - \frac{m_{\nu_\alpha}^2 + m_{\nu_\beta}^2}{2} \right) \right] \\ & \times \frac{1}{s_{j\alpha}} \sqrt{(s_{j\alpha} - m_{\ell_j}^2 - m_{\nu_\alpha}^2)^2 - 4m_{\nu_\alpha}^2 m_{\ell_j}^2} \sqrt{(m_{\ell_i}^2 + m_{\nu_\beta}^2 - s_{j\alpha})^2 - 4m_{\nu_\beta}^2 m_{\ell_i}^2} \\ & + \alpha \leftrightarrow \beta, \end{aligned} \quad (23)$$

where U is the full leptonic mixing matrix defined in Eq. (1) and G_F is the Fermi constant. The Dalitz variable is defined as $s_{j\alpha} = (p_{\ell_j} + p_{\nu_\alpha})^2$, p_{ℓ_j} , p_{ν_α} being the corresponding momenta for ℓ_j and ν_α .

Mesonic τ decays

It is also interesting to consider the impact of the modified $W\ell\nu$ vertex on mesonic τ decays. In particular, we consider the following observables

$$R_K^{\ell\tau} \equiv \frac{\Gamma(\tau \rightarrow K\nu)}{\Gamma(K \rightarrow \ell\nu)} \quad \text{and} \quad R_\pi^{\ell\tau} \equiv \frac{\Gamma(\tau \rightarrow \pi\nu)}{\Gamma(\pi \rightarrow \ell\nu)}, \quad (24)$$

with $\ell = e, \mu$. These observables allow to indirectly probe the universality of the τ -coupling, while remaining free of hadronic matrix element uncertainties. Indeed, the dependence on the decay constants cancels out in these ratios at tree-level. The corresponding experimental values can be computed from the individual decay widths given in [24]

$$R_K^{\mu\tau} = 469.3 \pm 7.0 \quad \text{and} \quad R_\pi^{\mu\tau} = 9703 \pm 34, \quad (25)$$

$$R_K^{e\tau} = (1.886 \pm 0.078) \times 10^7 \quad \text{and} \quad R_\pi^{e\tau} = (7.888 \pm 0.038) \times 10^7, \quad (26)$$

while our estimations of the tree-level SM predictions are

$$R_K^{\mu\tau} = 476.0 \quad \text{and} \quad R_\pi^{\mu\tau} = 9756, \quad (27)$$

$$R_K^{e\tau} = 1.853 \times 10^7 \quad \text{and} \quad R_\pi^{e\tau} = 7.602 \times 10^7. \quad (28)$$

In the SM extended by the new sterile states, the mesonic τ decay width is given by

$$\Gamma(\tau \rightarrow P\nu_i) = \frac{G_F^2 f_P^2}{16\pi m_\tau^3} |U^{3i}|^2 |V_{\text{CKM}}^{qq'}|^2 \lambda^{1/2}(m_\tau, m_P, m_{\nu_i}) [(m_\tau^2 - m_{\nu_i}^2)^2 - m_P^2(m_{\nu_i}^2 + m_\tau^2)], \quad (29)$$

⁵New corrections to the SM results for the leptonic decay width of muons and taus have been recently discussed in [51, 52], in the limit of massless neutrinos.

where $P = \pi, K$ and $i = 1, \dots, N_{\max}^{(P)}$. The function $\lambda(m_\tau, m_P, m_{\nu_i})$ has been given in Eq. (12) and $V_{\text{CKM}}^{qq'}$ denotes the appropriate CKM matrix element. In addition, $N_{\max}^{(P)}$ is the heaviest neutrino mass eigenstate which is kinematically allowed when a P meson is produced. The leptonic pseudoscalar meson decay width in the presence of additional sterile neutrinos was given in [7], and will be discussed in the following subsection (see Eqs. (30, 32)).

3.3 Leptonic pseudoscalar meson decays

We now address the decays of pseudoscalar mesons into leptons, whose dominant contributions arise from tree-level W mediated exchanges. The theoretical prediction of some decays can be plagued by hadronic matrix element uncertainties (as is the case of leptonic B decays): however, by considering the ratios

$$R_P \equiv \frac{\Gamma(P^+ \rightarrow e^+ \nu)}{\Gamma(P^+ \rightarrow \mu^+ \nu)}, \quad (30)$$

these can be significantly reduced since the hadronic uncertainties cancel out to a good approximation, so that the SM predictions can be computed with a high precision. In order to compare the experimental bounds (some of which have recently been obtained with an impressive precision) with the SM expectation, it proves convenient to use the quantity Δr_P , which parametrises deviation from the SM prediction, possibly arising from new physics contributions:

$$R_P = R_P^{\text{SM}} (1 + \Delta r_P) \quad \text{or equivalently} \quad \Delta r_P \equiv \frac{R_P}{R_P^{\text{SM}}} - 1. \quad (31)$$

The expression for R_P in the SM extended by sterile neutrinos is given by [7]

$$R_P = \frac{\sum_i F^{i1} G^{i1}}{\sum_k F^{k2} G^{k2}}, \quad \text{with} \quad (32)$$

$$F^{ij} = |U^{ji}|^2 \quad \text{and} \quad G^{ij} = \left[m_P^2 (m_{\nu_i}^2 + m_{\ell_j}^2) - (m_{\nu_i}^2 - m_{\ell_j}^2)^2 \right] \lambda^{1/2}(m_P, m_{\nu_i}, m_{\ell_j}), \quad (33)$$

where the function $\lambda(m_P, m_{\nu_i}, m_{\ell_j})$ is given by Eq. (12). Again, we recall that all states do not necessarily contribute to R_P ; this can be confirmed from inspection of G^{ij} , which must be a positive definite quantity.

The result of Eq. (32) allows for a straightforward interpretation of the impact of the new sterile states: F^{ij} represents the impact of new interactions (absent in the SM), whereas G^{ij} encodes the mass-dependent factors. In the limit where $m_{\nu_i} = 0$ and $U^{ji} = \delta_{ji}$, one can recover the SM result from Eq. (32),

$$R_P^{\text{SM}} = \frac{m_e^2 (m_P^2 - m_e^2)^2}{m_\mu^2 (m_P^2 - m_\mu^2)^2}, \quad (34)$$

to which small electromagnetic corrections (accounting for internal bremsstrahlung and structure-dependent effects) should be added [53]. Notice the strong helicity suppression, $R_P^{\text{SM}} \propto \frac{m_e^2}{m_\mu^2}$ in Eq.(34). This makes R_P (and Δr_P) one of the most sensitive observables to study lepton flavour universality violation.

The general expression for Δr_P reads

$$\Delta r_P = \frac{m_\mu^2 (m_P^2 - m_\mu^2)^2}{m_e^2 (m_P^2 - m_e^2)^2} \frac{\sum_{m=1}^{N_{\max}^{(e)}} F^{m1} G^{m1}}{\sum_{n=1}^{N_{\max}^{(\mu)}} F^{n2} G^{n2}} - 1, \quad (35)$$

where $N_{\max}^{(\ell_j)}$ is the heaviest neutrino mass eigenstate kinematically allowed in association with ℓ_j . As can be seen from the above equation, Δr_P can considerably deviate from zero, due to the mass hierarchy of the new states and the active-sterile mixings. Owing to its analytical transparency, we again stress the distinct sources of enhancement to Δr_P . Firstly, and if the new sterile states are light (in particular lighter than the decaying meson) all the ν_i mass eigenstates can be kinematically accessible as final states. Although in this limit unitarity would be recovered (as one would sum over all $3 + N_s$ states whose mixing is parametrised by U), Δr_P can still be enhanced due to the new phase space factors, see Eq. (33). Heavier steriles can also lead to an enhancement of Δr_P , as a result of deviations from unitarity: even though this is more model-dependent, sterile mixings to active neutrinos can be sizable due to the possibility of having larger Yukawa couplings.

Although the general expression for the leptonic pseudoscalar decays has been given above, Eqs. (32, 35), we briefly comment below on each of the specific observables we will address.

Light mesons: $R_{K,\pi}$ and $R_{e,\mu}$

The $R_{K,\pi}$ (and $\Delta r_{K,\pi}$) observables were already discussed in [7], and constitute a perfect test of lepton flavour universality. The comparison of theoretical analyses [53, 54] with the recent measurements from the NA62 collaboration [55, 56] and with the existing measurements on pion leptonic decays [57]

$$R_K^{\text{SM}} = (2.477 \pm 0.001) \times 10^{-5}, \quad R_K^{\text{Exp}} = (2.488 \pm 0.010) \times 10^{-5}, \quad (36)$$

$$R_\pi^{\text{SM}} = (1.2354 \pm 0.0002) \times 10^{-4}, \quad R_\pi^{\text{Exp}} = (1.230 \pm 0.004) \times 10^{-4}, \quad (37)$$

suggests that observation agrees at the 1σ level with the SM predictions for

$$\Delta r_K = (4 \pm 4) \times 10^{-3}, \quad \Delta r_\pi = (-4 \pm 3) \times 10^{-3}. \quad (38)$$

The current experimental uncertainty in Δr_K (of around 0.4%) should be further reduced in the near future, as one expects to have $\delta R_K/R_K \sim 0.1\%$ [58, 59], which can translate into measuring deviations $\Delta r_K \sim \mathcal{O}(10^{-3})$. There are also plans for a more precise determination of Δr_π [60, 61].

We also consider the observables

$$R_e \equiv \frac{\Gamma(\pi^+ \rightarrow e^+\nu)}{\Gamma(K^+ \rightarrow e^+\nu)}, \quad R_\mu \equiv \frac{\Gamma(\pi^+ \rightarrow \mu^+\nu)}{\Gamma(K^+ \rightarrow \mu^+\nu)}, \quad (39)$$

as well as the corresponding deviations from the SM predictions

$$R_{e,\mu} = R_{e,\mu}^{\text{SM}} (1 + \Delta r_{e,\mu}) \quad \text{or equivalently} \quad \Delta r_{e,\mu} \equiv \frac{R_{e,\mu}}{R_{e,\mu}^{\text{SM}}} - 1. \quad (40)$$

Although at first sight apparently redundant, the study of the observables $R_{e,\mu}$ and $\Delta r_{e,\mu}$ is well motivated. Indeed, they offer the possibility to extract the ratios f_π/f_K and $|V_{us}|/|V_{ud}|$ using an experimentally clean signal and with little theoretical uncertainty. Unfortunately, the current values of R_e and R_μ are at present computed using different measurements [24] coming from experiments that are sometimes separated by more than 20 years. This makes a proper evaluation of systematic uncertainties quite difficult. However, the NA62 experiment will have a good control of the systematics due to the presence of the same charged lepton in the final state (owing to the acquisition of both samples in the same data taking, with the same beam configuration and with

the same trigger strategy). In fact, R_e can be measured with a precision at the level of 0.5% within a few years at NA62 [62]. Even if the experimental prospects for R_μ are less appealing, we nevertheless include it for completeness in our study. The corresponding current experimental values are [24]

$$R_e = 3.70 \pm 0.02 \quad , \quad R_\mu = 0.748 \pm 0.002 \quad , \quad (41)$$

and these can be combined with our estimates of the SM results (central values),

$$R_e^{\text{SM}} = 3.71258 \quad , \quad R_\mu^{\text{SM}} = 0.743103 \quad , \quad (42)$$

leading to

$$\Delta r_e = -0.003 \pm 0.006 \quad , \quad \Delta r_\mu = 0.007 \pm 0.002 \quad . \quad (43)$$

Charmed mesons D, D_s : R_{D, D_s} and $R_{D_s}^D$

Nominal SM expectations on D and D_S leptonic decays, as well as the experimental results from CLEO-c and BES III, can be found in [63]. In our study we focus in particular on D_s observables, which have recently been well measured by CLEO-c [64]:

$$\begin{aligned} \text{BR}(D_s \rightarrow \tau^+ \nu) &= (5.52 \pm 0.57 \pm 0.21) \times 10^{-2} \quad , \\ \text{BR}(D_s \rightarrow \mu^+ \nu) &= (0.576 \pm 0.045 \pm 0.054) \times 10^{-2} \quad . \end{aligned} \quad (44)$$

Both these observables present a deviation from the theoretical expectation: 2.4 σ using the QCD sum rules estimation for the decay constant f_{D_s} , or a 2.8 σ deviation using the lattice determination (see [64] and references therein).

As before, considering ratios of decay widths (R_{D_s}) allows to cancel the theoretical uncertainties (due to f_{D_s}), and thus to compute the SM prediction to a high precision,

$$R_{D_s} \equiv \frac{\Gamma(D_s \rightarrow \tau \nu)}{\Gamma(D_s \rightarrow \mu \nu)} \quad . \quad (45)$$

Motivated by the fact that the ratio of D_s and D decay constants was recently determined to a high precision [65], we have also studied the following ratio

$$R_{D_s^D} \equiv \frac{\Gamma(D_s \rightarrow \tau \nu)}{\Gamma(D \rightarrow \mu \nu)} \propto \frac{1}{\lambda^2} \left| \frac{f_{D_s}}{f_D} \right|^2 \quad , \quad (46)$$

where λ is the CKM parameter in the Wolfenstein parametrisation ($V_{\text{CKM}}^{cs}/V_{\text{CKM}}^{cd} = 1/\lambda$) and f_{D_s} , f_D are the D_s and D pseudoscalar decay constants, respectively. Lattice QCD computations have allowed to determine the ratio f_{D_s}/f_D with a high precision. For instance in [66], one has

$$\frac{f_{D_s}}{f_D} = 1.187 \pm 0.012 \quad , \quad (47)$$

while in [65], one has

$$\frac{f_{D_s}}{f_D} = 0.995(6)(4) \times \frac{f_K}{f_\pi} \quad , \quad (48)$$

f_K and f_π being the kaon and pion decay constants, whose ratio is given by (world average value, see [67]):

$$\frac{f_K}{f_\pi} = 1.194(5) \quad . \quad (49)$$

Leptonic B meson decays: $\text{BR}(B \rightarrow \tau\nu)$

Similarly, the leptonic decays of heavier mesons can also be affected by changes in the $W\ell\nu$ vertex, in particular $B \rightarrow \tau\nu$. In the SM extended by the new sterile states, the decay rate for $B \rightarrow \tau\nu_i$ is given by:

$$\Gamma(B \rightarrow \tau\nu_i) = \frac{G_F^2 f_B^2}{8\pi m_B^3} |U^{3i}|^2 |V_{\text{CKM}}^{ub}|^2 \lambda^{1/2}(m_B, m_\tau, m_{\nu_i}) [m_B^2(m_{\nu_i}^2 + m_\tau^2) - (m_\tau^2 - m_{\nu_i}^2)^2] , \quad (50)$$

where $i = 1, \dots, N_{\text{max}}$ (N_{max} corresponding to the heaviest ν_s which is kinematically allowed when the B meson decays into a τ lepton). The function $\lambda(m_B, m_\tau, m_{\nu_i})$ has been given in Eq. (12).

The following bounds must be taken into account [24]:

$$\text{BR}(B \rightarrow e\nu) < 9.8 \times 10^{-7} , \quad (51)$$

$$\text{BR}(B \rightarrow \mu\nu) < 10^{-6} , \quad (52)$$

$$\text{BR}(B \rightarrow \tau\nu) = (1.65 \pm 0.34) \times 10^{-4} . \quad (53)$$

It should be noted that the experimental measurement of $\text{BR}(B \rightarrow \tau\nu)$ significantly deviates from its SM prediction,

$$\text{BR}^{\text{SM}}(B \rightarrow \tau\nu) = (0.83(8)(6)) \times 10^{-4} , \quad (54)$$

which was obtained with $V_{\text{CKM}}^{ub} = 3.65(13) \times 10^{-3}$, corresponding to the average estimate from the global fits of CKMfitter [68] and UTfit [69], and $f_B = (188 \pm 6)$ MeV, an average from the most recent lattice QCD results [70–72]. Interestingly, the Belle collaboration has published an updated analysis, reporting an even lower value [73],

$$\text{BR}(B \rightarrow \tau\nu) = (0.72_{-0.25}^{+0.27} \pm 0.11) \times 10^{-4} , \quad (55)$$

and when averaged with the BaBar result [74], the Belle measurement leads to

$$\text{BR}(B \rightarrow \tau\nu) = (1.15 \pm 0.23) \times 10^{-4} . \quad (56)$$

Notice that since only the decay $B \rightarrow \tau\nu$ has been observed, it is not possible to study a ratio of decay widths as done for other pseudoscalar mesons.

3.4 Semileptonic pseudoscalar meson decays

Recent (surprising) experimental results for the ratio of the branching fractions of the $B \rightarrow D^{(*)}\tau\nu$ and $B \rightarrow D^{(*)}\mu\nu$ decays have opened the door to the possibility of constraining potential New Physics contributions through these decay modes. In our analysis, we only focus on the following observable⁶

$$R(D) \equiv \frac{\text{BR}(B^+ \rightarrow D\tau^+\bar{\nu}_\tau)}{\text{BR}(B^+ \rightarrow D\mu^+\bar{\nu}_\mu)} , \quad (57)$$

for which BaBar's recent measurement [75] is

$$R(D)^{\text{Exp}} = 0.440 \pm 0.058_{\text{stat.}} \pm 0.042_{\text{syst.}} . \quad (58)$$

Notice that BaBar's definition of $R(D)$ does not distinguish a muon from an electron in the final state, i.e., the observable in fact corresponds to $R(D) = \frac{\Gamma(B^+ \rightarrow D\tau^+\nu)}{\Gamma(B^+ \rightarrow D\ell^+\nu)}$.

⁶We recall that the form factors for $B \rightarrow D^*\ell\nu$ are poorly known and have very large theoretical uncertainties.

Based on lattice estimations of the hadronic matrix elements (parametrised by form factors), the SM prediction for $R(D)$ is [76]

$$R(D)^{\text{SM}} = 0.31 \pm 0.02, \quad (59)$$

which lies more than 1σ (but less than 2σ) below the experimental results⁷.

It is worth mentioning that the BaBar excess of events in $B \rightarrow D^* \tau \nu$ decays, revealing a 3.4σ deviation from the SM prediction [78], cannot be accommodated by contributions from charged Higgs bosons in the context of type-II Two Higgs Doublet Model (2HDM) [79]. In fact, BaBar excludes the latter contributions as an explanation of the deviations in $R(D)$ and $R(D^*)$ from their SM predictions [80]. Moreover, and as discussed in [81], the observed excess on $R(D)$ (and $R(D^*)$) also fails to be explained in large portions of the more general type-III 2HDM. Similarly, the authors of Ref. [79] found regions in the parameter space of the Aligned 2HDM able to accommodate the $R(D^*)$ measurement, although in conflict with the constraints from leptonic charm decays.

For these observables, the mass of the neutral leptons is usually neglected. Here we will derive analytical expressions for $\Gamma(P \rightarrow P' + \ell_i + \nu_j)$ in terms of invariants, keeping all lepton masses (neutral and charged ones). Notice that $R(D)$ is more interesting since tests of compatibility of the Standard Model (or any of its extensions) can be done experimentally with a *minimal theory input*. Indeed, the decay rates are parametrised by two form factors, $F^+(q^2)$ and $F^0(q^2)$. The first, $F^+(q^2)$, has recently been experimentally well measured [82] and the behaviour of the second, $F^0(q^2)$, with respect to the transfer momentum q^2 , has also been determined [76] (consistent with many different theoretical estimations from Lattice QCD collaborations [83, 84], as well as with QCD sum rules analyses [85, 86]),

$$\frac{F^0(q^2)}{F^+(q^2)} = 1 - \alpha q^2, \quad \alpha = 0.022(1) \text{ GeV}^{-2}. \quad (60)$$

Consider then the semileptonic meson decay

$$P \rightarrow P' + \ell_i + \nu_j, \quad (61)$$

with m the mass of the decaying pseudoscalar meson, $m_{1,2}$ those of the final state charged and neutral leptons, and m_3 the mass of the final pseudoscalar state meson. The total width of the decay can be decomposed as

$$\Gamma_{\text{tot}} = \Gamma_{c_1} + \Gamma_{c_2} + \Gamma_{c_3} + \Gamma_{c_4}, \quad (62)$$

where each (partial) width is associated to the form factors $F^+(q^2)$, $F^0(q^2)$ (and combinations thereof) as follows

$$\Gamma_{c_1, c_2} \rightsquigarrow |F^+(q^2)|^2; \quad \Gamma_{c_3} \rightsquigarrow |F^0(q^2)|^2; \quad \Gamma_{c_4} \rightsquigarrow 2 \text{Re}(F^0 F^{+*}). \quad (63)$$

⁷This SM estimation is consistent with a different theoretical prediction made in [77].

The above widths can be written as:

$$\begin{aligned}
\Gamma_{c_1} &= \frac{G_F^2}{192\pi^3} \frac{|V_{\text{CKM}}^{qq'}|^2 |U_{ij}|^2}{m^3} \int_{(m_1+m_2)^2}^{(m-m_3)^2} dq^2 |F^+(q^2)|^2 \lambda^{3/2}(q, m, m_3) \lambda^{3/2}(q, m_1, m_2) \frac{1}{q^6}, \\
\Gamma_{c_2} &= \frac{G_F^2}{128\pi^3} \frac{|V_{\text{CKM}}^{qq'}|^2 |U_{ij}|^2}{m^3} \int_{(m_1+m_2)^2}^{(m-m_3)^2} dq^2 |F^+(q^2)|^2 \lambda^{3/2}(q, m, m_3) \lambda^{1/2}(q, m_1, m_2) \frac{1}{q^6} \times \\
&\quad [q^2(m_1^2 + m_2^2) - (m_1^2 - m_2^2)^2], \\
\Gamma_{c_3} &= \frac{G_F^2}{128\pi^3} \frac{|V_{\text{CKM}}^{qq'}|^2 |U_{ij}|^2}{m^3} \int_{(m_1+m_2)^2}^{(m-m_3)^2} dq^2 |F^0(q^2)|^2 \left(\frac{\Delta m^2}{q^2}\right)^2 \lambda^{1/2}(q, m, m_3) \frac{1}{q^2} \times \\
&\quad \lambda^{1/2}(q, m_1, m_2) [q^2(m_1^2 + m_2^2) - (m_1^2 - m_2^2)^2], \\
\Gamma_{c_4} &= 0.
\end{aligned} \tag{64}$$

In the above expressions, $V_{\text{CKM}}^{qq'}$ denotes the appropriate CKM matrix element, q the momentum transfer, Δm^2 refers to the squared mass difference between the two meson masses

$$\Delta m^2 = m^2 - m_3^2, \tag{65}$$

and the function $\lambda(q, m_1, m_2)$ is given by Eq. (12).

4 Numerical results and discussion

As mentioned before, the non-unitarity of the leptonic mixing matrix, together with the possible phase space enhancement (when the sterile states are very light), can modify the contributions to rates for leptonic and hadronic processes with neutrinos in the final state. Observables which have been measured with very good precision, and are in agreement with SM expectations, will allow to constrain the departure from $\sum_i |U^{ji}|^2 = 1$ (as seen in Section 3.3, the observables depend on $\sum_i |U^{ji}|^2$, with the sum extending over all kinematically accessible neutrino states).

In our approach we assume that all NP effects lie in the lepton sector; notice however, that the decorrelation of NP effects arising from the modified $W\ell\nu$ vertex is sometimes hampered by large systematic uncertainties on the hadronic matrix elements (with impact on V_{CKM} element determination). Moreover, as already mentioned, we do not address higher-order corrections (had we computed the latter, the systematic errors related to the uncertainty in hadronic matrix elements would overlap with our own systematics).

Although the generic idea explored in this work applies to any model where the active neutrinos have sizable mixings with some additional singlet states, in order to evaluate the contributions of the new states, one must consider a specific framework. Here, as an illustrative example, we consider the case of the Inverse Seesaw [12] to discuss the potential of a model with sterile neutrinos regarding tree-level contributions to leptonic and semileptonic meson decays (as mentioned before, there are other possible frameworks to illustrate the effect of sterile neutrinos on these observables).

4.1 The inverse seesaw

In the inverse seesaw [12], the SM particle content is extended by n_R generations of right-handed (RH) neutrinos ν_R and n_X generations of singlet fermions X (such that $n_R + n_X = N_s$), both with lepton number $L = +1$ [12]. Even if deviations from unitarity can occur for different values of n_R and n_X , here we will consider the case $n_R = n_X = 3$. The Lagrangian is given by

$$\mathcal{L}_{\text{ISS}} = \mathcal{L}_{\text{SM}} - Y_{ij}^\nu \bar{\nu}_{Ri} \tilde{H}^\dagger L_j - M_{Rij} \bar{\nu}_{Ri} X_j - \frac{1}{2} \mu_{Xij} \bar{X}_i^c X_j + \text{h.c.}, \tag{66}$$

where $i, j = 1, 2, 3$ are generation indices and $\tilde{H} = i\sigma_2 H^*$. Notice that the present lepton number assignment for the new states, together with $L = +1$ for the SM lepton doublet, implies that the Dirac-type right-handed neutrino mass term M_{Rij} conserves lepton number, while the Majorana mass term μ_{Xij} violates it by two units.

The non-trivial structure of the neutrino Yukawa couplings Y^ν implies that the left-handed neutrinos mix with the right-handed ones after electroweak symmetry breaking. In the $\{\nu_L, \nu_R^c, X\}$ basis, one has the following symmetric (9×9) mass matrix \mathcal{M} ,

$$\mathcal{M} = \begin{pmatrix} 0 & m_D^T & 0 \\ m_D & 0 & M_R \\ 0 & M_R^T & \mu_X \end{pmatrix}. \quad (67)$$

Here $m_D = \frac{1}{\sqrt{2}} Y^\nu v$, $v/\sqrt{2}$ being the vacuum expectation value of the SM Higgs boson. Assuming $\mu_X \ll m_D \ll M_R$, the diagonalization of \mathcal{M} leads to an effective Majorana mass matrix for the active (light) neutrinos [87],

$$m_\nu \simeq m_D^T M_R^{T-1} \mu_X M_R^{-1} m_D, \quad (68)$$

while the remaining 6 sterile states have masses approximately given by $M_\nu \simeq M_R$.

In what follows, and without loss of generality, we work in a basis where M_R is a diagonal matrix (as are the charged lepton Yukawa couplings). The couplings Y^ν can be written using a modified Casas-Ibarra parametrisation [88] (thus automatically complying with light neutrino data):

$$Y^\nu = \frac{\sqrt{2}}{v} D^\dagger \sqrt{\hat{M}} R \sqrt{\hat{m}_\nu} U_{\text{PMNS}}^\dagger, \quad (69)$$

where $\sqrt{\hat{m}_\nu}$ is a diagonal matrix containing the square roots of the three eigenvalues of m_ν (cf. Eq. (68)); likewise $\sqrt{\hat{M}}$ is a diagonal matrix with the square roots of the eigenvalues of $M = M_R \mu_X^{-1} M_R^T$. The matrix D diagonalizes M as $D M D^T = \hat{M}$, and R is a 3×3 complex orthogonal matrix, parametrised by 3 complex angles, encoding the remaining degrees of freedom.

A distinctive feature of the ISS is that the additional μ_{Xij} parameters allow to accommodate the smallness of the active neutrino masses m_ν for a low seesaw scale, but still with natural Yukawa couplings ($Y^\nu \sim \mathcal{O}(1)$). As a consequence, one can have sizable mixings between the active neutrinos and the additional sterile states. This is in contrast with the canonical type-I seesaw, where having $\mathcal{O}(1)$ Yukawa couplings usually requires $M_R \sim 10^{15}$ GeV, thus leading to truly negligible active-sterile mixings.

The neutrino mass matrix is diagonalized as $U_\nu^T \mathcal{M} U_\nu = \text{diag}(m_i)$. The nine neutrino mass eigenstates enter the leptonic charged current through their left-handed component (see Eq. (1), with $i = 1, \dots, 9$, $j = 1, \dots, 3$). Again in the basis where the charged lepton mass matrix is diagonal, the leptonic mixing matrix U is given by the the rectangular 3×9 sub-matrix corresponding to the first three columns of U_ν .

Finally, we also refer to [89–91] for earlier studies on non-unitarity effects in the inverse seesaw.

4.2 Constraining the ISS parameter space

The adapted Casas-Ibarra parametrisation for Y^ν , Eq. (69), ensures that neutrino oscillation data is satisfied (we use the best-fit values of the global analysis of [16] - see Eqs. (6, 7)). The R matrix angles are taken to be real, their value randomly varied in the range $\theta_i \in [0, 2\pi]$ (thus no contributions to lepton electric dipole moments are expected). However, we have verified that similar results are found when considering the more general complex R matrix case. We also

study both hierarchies for the light neutrino spectrum, and the effect of a non-vanishing Dirac CP violating phase.

The simulated points are then subject to all the constraints previously mentioned, and those not complying with the different bounds (with the exception of the cosmological constraints) are excluded. As argued in [42], the cosmological bounds can be evaded by considering a non-standard-cosmology; we therefore keep these points, explicitly identifying them via a distinctive colour scheme (blue points in agreement with cosmological bounds, red points requiring a non-standard cosmology) throughout the numerical analysis and subsequent discussion. For illustrative purposes, we also display points excluded by the recent MEG bound (see Eq. 14)), although these will always be identified by a different colour scheme (grey points in this case).

Before proceeding to the analysis of the observables, let us briefly discuss the effect of the above mentioned constraints on the potential deviations from unitarity of the \tilde{U}_{PMNS} matrix, which is parametrised by $\tilde{\eta}$

$$\tilde{\eta} = 1 - |\text{Det}(\tilde{U}_{\text{PMNS}})|, \quad (70)$$

considering both cases of normal (NH) and inverted (IH) hierarchies for the light neutrino spectrum.

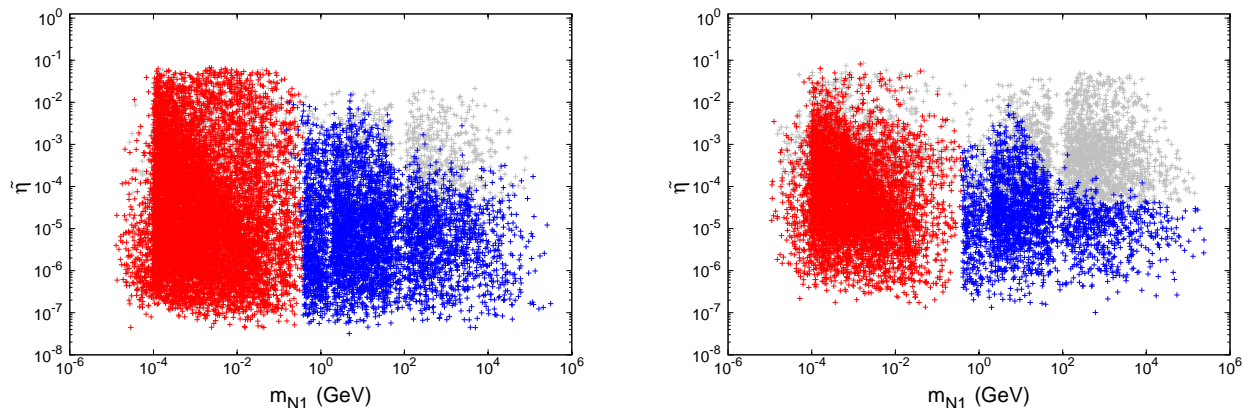


Figure 1: Deviation from unitarity of the \tilde{U}_{PMNS} matrix, parametrised by $\tilde{\eta}$, as a function of the lightest sterile neutrino mass, m_{N_1} , for normal (left) and inverted hierarchical (right) light neutrino spectra. Blue points are in agreement with cosmological bounds, while the red ones would require considering a non-standard cosmology. Grey points correspond to an associated $\text{BR}(\mu \rightarrow e\gamma)$ already excluded by MEG.

As can be seen from Fig. 1, regimes of $\tilde{\eta} \sim \mathcal{O}(10^{-1})$ are indeed possible; however these solutions are typically disfavoured from standard cosmology arguments. It is nevertheless clear that the ISS framework favours a NH scheme (notice that the density of points surviving the above mentioned constraints is denser in this case). Moreover, the recent MEG bound has a more severe impact in the case of IH scheme, excluding larger portions of the parameter space (here illustrated in the $\tilde{\eta} - m_{N_1}$ plane). Notice that values $\tilde{\eta} \gtrsim \mathcal{O}(10^{-1})$ are excluded since in this limit the seesaw condition is not satisfied.

The prospects concerning the observation of $\text{BR}(\mu \rightarrow e\gamma)$ at MEG, as well as the impact of the current bound regarding the parameter space surveyed in our analysis, are collected in Fig. 2.

Given the significant constraints on the parameter space arising from this observable, it would be undoubtably interesting to consider the actual impact of $\text{BR}(\mu \rightarrow e\gamma)$ on other parameters of the model, such as $\mu_{X_{ij}}$, or the active-sterile mixing angles $\theta_{i\alpha}$. However, and as can be inferred from the description of the underlying numerical scan, the fact that one has explored all degrees of freedom of the Yukawa couplings precludes this (for example, the impact of a given texture and/or regime for μ_X and M_R would be mitigated by the mixings introduced via the R -matrix). In other words, it is not possible to individually explore the effect of a given parameter on observables, as the latter simultaneously depend on a number of (varying) parameters. Likewise, considering the dependence of an observable on a given active-sterile mixing angle $\theta_{i\alpha}$ would provide little insight, as various physical mixing regimes arise from the scan.

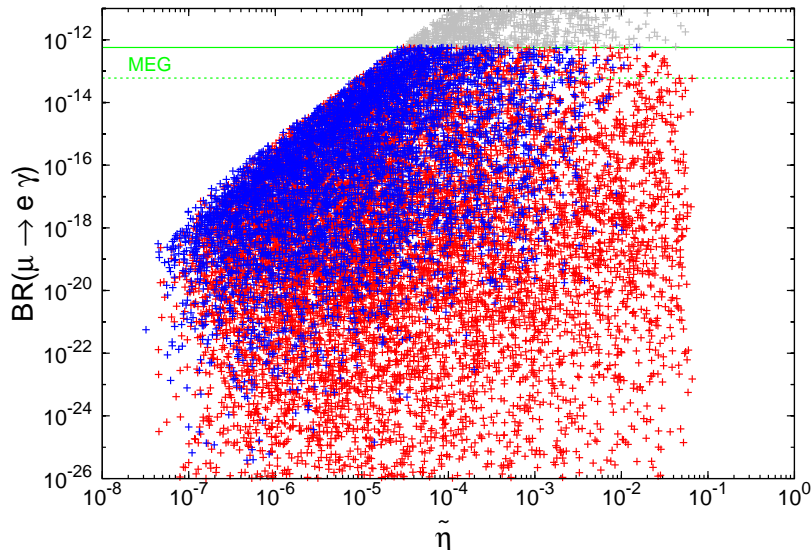


Figure 2: $\text{BR}(\mu \rightarrow e\gamma)$ as a function of $\tilde{\eta}$, for the case of a NH spectrum. Colour code as in Fig. 1. Green horizontal lines denote current experimental bounds (solid) and MEG future sensitivity [27] (dashed).

In what follows, we will consider a NH light neutrino spectrum in our analysis of the different observables. Unless otherwise stated, the Dirac CP violating phase δ will be set to zero.

4.3 Invisible Z decays and $W \rightarrow \ell\nu$

We begin our analysis by discussing the potential contributions of the additional sterile states to EW observables, in particular the invisible Z decay width (which is an EW precision test) and leptonic W decays.

On the left panel of Fig. 3, we display the invisible Z decay width, $\Gamma(Z \rightarrow \nu\nu)$ (see Eqs. (10-13)), as a function of $\tilde{\eta}$. A black horizontal line denotes the SM prediction (cf. Eq. (8)), while green lines (full/dashed/dotted) correspond to the experimental measurements from LEP (central, 1σ and 2σ intervals, respectively, see Eq. (9)). The apparent difference between the SM line (corresponding to a full computation of this observable) and our SM-limit (obtained for the regime of very small $\tilde{\eta}$, for which the PMNS becomes unitary) in Fig. 3 is due to the fact that the latter is based on a tree-level computation; should higher order corrections be taken into account, all

points would be shifted towards the SM theoretical prediction.

Clearly, and even though the non-unitarity of the PMNS only indirectly affects $Z \rightarrow \nu\nu$ decays (via the small sterile component in the active light neutrino eigenstates) this EW precision observable is a crucial consistency check of any model with extra sterile fermions, as the invisible decay width cannot exceed the SM prediction [22,23]. As can be seen in the left panel of Fig. 3, a sizable reduction of the invisible decay width could indeed occur for a regime of large $\tilde{\eta}$. However, this reduction of $\Gamma(Z \rightarrow \nu\nu)$ is precluded by the current MEG bound on $\text{BR}(\mu \rightarrow e\gamma)$.

These regimes of large $\tilde{\eta}$ are associated with large values of the Yukawa couplings Y_{ij}^ν : having such large values of Y_{ij}^ν for a comparatively low seesaw scale is a direct consequence of an inverse seesaw as the underlying framework for sterile neutrinos (this effect was already discussed in [7], in relation to LFU violation in light pseudoscalar meson decays). For $Y^\nu \sim \text{few} \times 10^{-2}$, large active-sterile mixings can occur, possibly leading to a decrease in the Z boson decay width (in agreement with [22,23]). This can be confirmed on the right panel of Fig. 3, where we display $\Gamma(Z \rightarrow \nu\nu)$ versus the corresponding largest entry of the neutrino Yukawa couplings, $\max(Y_{ij}^\nu)$.

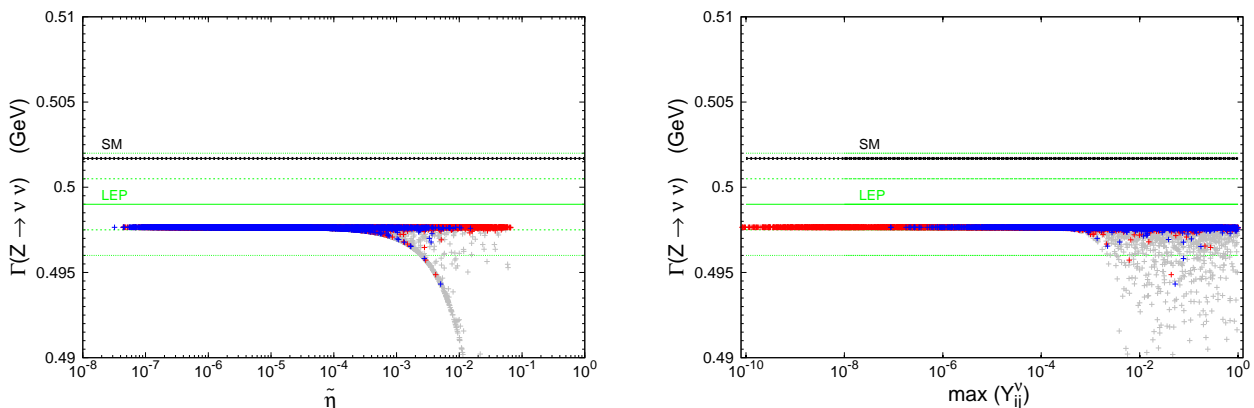


Figure 3: $\Gamma(Z \rightarrow \nu\nu)$ as a function of $\tilde{\eta}$ (on the left) and of the maximal entry of $Y_{ij}^\nu/4\pi$ (on the right). Blue points are in agreement with cosmological bounds, while the red ones would require considering a non-standard cosmology. Black lines denote the SM prediction, green ones correspond to the experimental measurement (full/dashed/dotted corresponding to central value, 1σ and 2σ intervals, respectively). Grey points correspond to an associated $\text{BR}(\mu \rightarrow e\gamma)$ already excluded by MEG.

We now proceed to address the impact of sterile neutrinos and the associated non-unitarity of the \tilde{U}_{PMNS} matrix on its most directly related observable: leptonic W decays. As mentioned in Section 3.1, there is at present a tension between the experimental determination of $\text{BR}(W \rightarrow \ell\nu)$ and the SM expectation, see Eqs. (17 - 19). In view of the sizable deviations that light sterile neutrinos can induce to (virtual) W mediated processes, we thus explore whether the additional states can have an impact on the decay BRs as well. In Fig. 4, we display $\text{BR}(W \rightarrow e\nu)$ and $\text{BR}(W \rightarrow \tau\nu)$, both as a function of $\tilde{\eta}$ (the behaviour of $\text{BR}(W \rightarrow \mu\nu)$ strongly resembles that of $\text{BR}(W \rightarrow e\nu)$, and we so refrain from displaying the corresponding plot). As can be seen from the left panel of Fig. 4, and similar to what occurred for the Z -decay width, non negligible contributions could indeed soften the tension between the SM prediction and the experimental values; however, the corresponding regime is excluded by current MEG bounds. In any case, a

simultaneous reconciliation of the tension for the three leptonic W branching ratios would not have been possible since, as can be seen from the right panel of Fig. 4, the non-unitarity of the PMNS matrix worsens the discrepancy for $\text{BR}(W \rightarrow \tau\nu)$. We notice that in the SM limit, corresponding to $\tilde{\eta} \sim 0$, there is a minor discrepancy between our values for the BRs and the SM line [45], since in our analysis we do not take into account higher-order corrections included in the SM prediction.

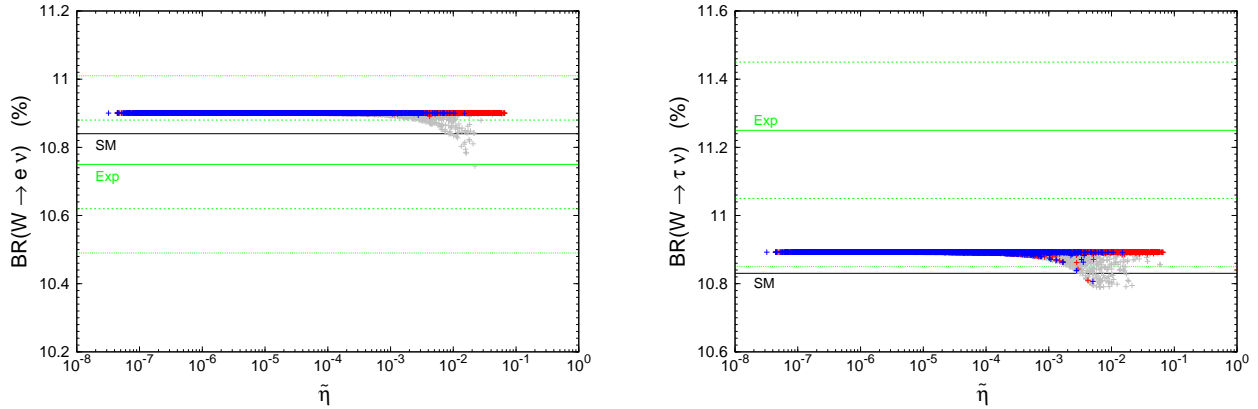


Figure 4: $\text{BR}(W \rightarrow \ell\nu)$ as a function of $\tilde{\eta}$. Colour code as in Fig. 3. Black lines denote the SM prediction, green ones correspond to the experimental measurement (full/dashed/dotted corresponding to central value, 1σ and 2σ intervals, respectively).

4.4 τ decays

The ratio of leptonic τ decays R_τ , defined in Eq. (20), could also be sensitive to deviations from unitarity. However, as seen in Fig. 5, the explored parameter space induces values for R_τ which are compatible with experimental CLEO and BaBar bounds at the (less than) 1σ level.

The ratios $R_K^{e\tau}$ and $R_\pi^{e\tau}$ defined in Eq. (24) might also be sensitive to deviations from unitarity. While the SM predictions are in good agreement with the experimental measurements for $R_K^{e\tau}$ (which can therefore be used to constrain deviations from unitarity), there is a discrepancy for $R_\pi^{e\tau}$. In Fig. 6 we display the non-unitarity effects: for $R_K^{e\tau}$, and although most of the points lie within the experimental 2σ interval, some exhibit a considerable reduction; a similar situation occurs for $R_\pi^{e\tau}$ (notice however that the observed deviation does not alleviate the aforementioned tension). From both cases, it is also clear that departures from the SM-like limit mostly occur for points already disfavoured by standard cosmology. We have also considered $R_K^{\mu\tau}$ and $R_\pi^{\mu\tau}$ and found a fair agreement between experimental values and theoretical predictions. However, it is important to stress that no single experiment directly measures $R_K^{\mu\tau}$ or $R_\pi^{\mu\tau}$. Moreover, and since some of the measurements are separated in time by more than five years, there might be systematics coming from the combination of different experimental results. A detailed analysis of these possible systematics is beyond the scope of this work. Nevertheless, a direct experimental measurement of the ratios $R_P^{\ell\tau}$ would avoid these issues: this could be achieved by considering the decay chain $\tau \rightarrow P(\rightarrow \ell\nu)\nu$ and measuring simultaneously $\text{BR}(\tau \rightarrow P\nu)$ and $\text{BR}(\tau \rightarrow P\nu) \times \text{BR}(P \rightarrow \ell\nu)$.

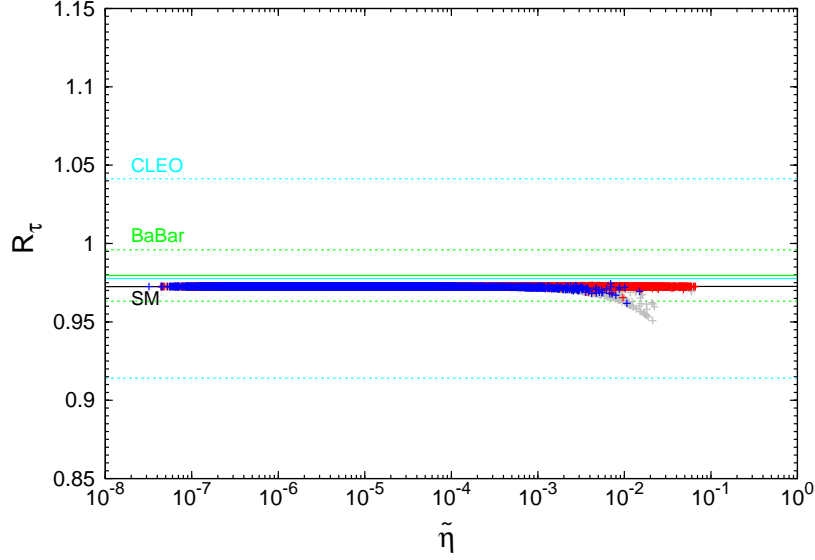


Figure 5: R_τ as a function of $\tilde{\eta}$. Colour code as in Fig. 3. In this case, green/cyan lines denote the BaBar/CLEO experimental measurements (full and dashed lines corresponding to central values and 1σ interval, respectively).

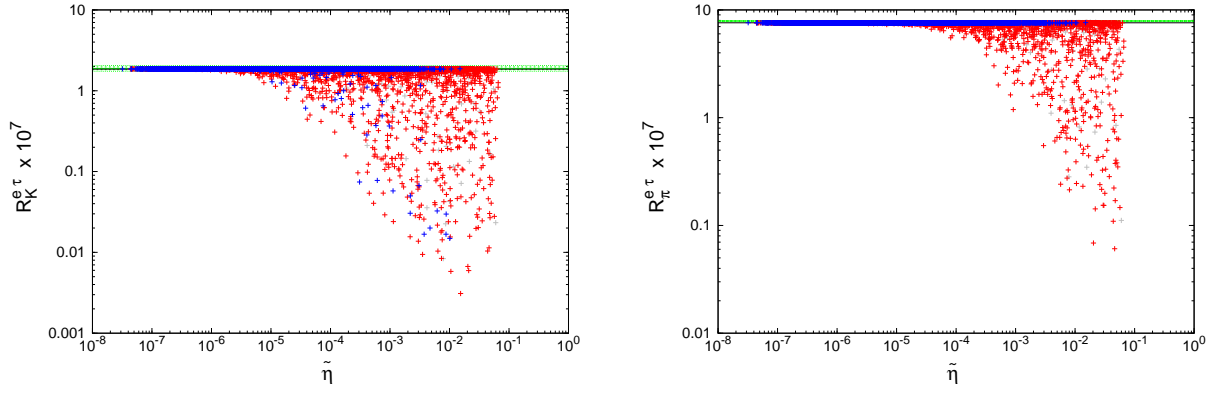


Figure 6: Ratios of τ mesonic and pseudoscalar leptonic decay widths, $R_{K,\pi}^{e\tau}$, as a function of $\tilde{\eta}$. Line and colour code as in Fig. 3.

4.5 Leptonic pseudoscalar meson decays

We now consider the impact of the non-unitarity of the PMNS matrix, as well as of having light sterile neutrino final states, regarding several observables related to leptonic pseudoscalar meson decays.

Light meson decays - $R_{K,\pi}$ and $\Delta r_{K,\pi}$

We begin by discussing the violation of lepton flavour universality in light pseudoscalar meson decays⁸, parametrised by $\Delta r_{K,\pi}$ as defined in Eq. (31). We display the results in Figs. 7 and 8.

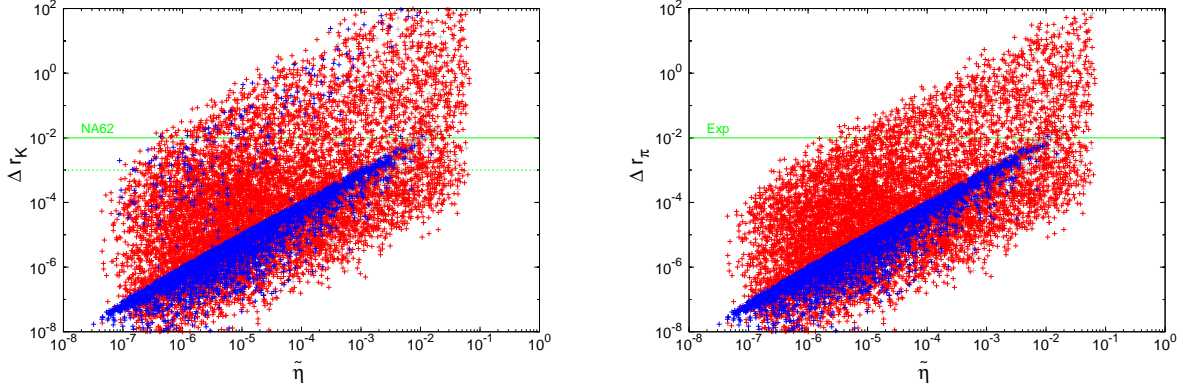


Figure 7: Δr_K and Δr_π (respectively left and right panels) as a function of $\tilde{\eta}$. Colour code as in Fig. 3. A full green line denotes the experimental upper bound (for Δr_K a green dashed line denotes the NA62 expected future sensitivity).

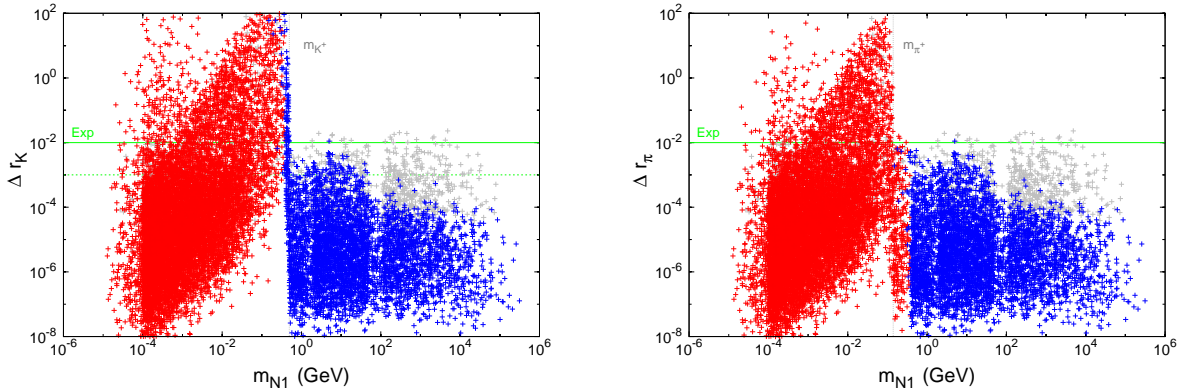


Figure 8: Δr_K and Δr_π (respectively left and right panels) as a function of the lightest sterile neutrino mass, m_{N_1} . Colour code as in Fig. 3. Full green lines denote the experimental upper bound (for Δr_K a green dashed line denotes the NA62 expected future sensitivity). Grey vertical dashed lines denote thresholds associated with the decaying meson mass, respectively m_{K^+} and m_{π^+} .

Even under the strong constraints arising from the recent MEG bound, one still recovers the results formerly obtained in [7]: as seen in Fig. 7, large deviations from the SM prediction, within experimental sensitivity, can be found.

⁸The rôle of R_π in probing non-standard axial and pseudoscalar interactions has recently been explored using an effective approach in [92].

Figure 8 also offers a clear insight into the different thresholds related to the decaying meson mass, and the associated source of deviation from the SM: as discussed in Section 3.3, and as explicitly shown in Eq. (33), for sterile neutrinos lighter than the decaying meson, one can have sizable deviations from the SM, since phase space factors considerably enhance the effects of any deviation from unitarity of U_{PMNS} (even if in some case unitarity can be approximately recovered). For kaons, and contrary to what occurs for the (lighter) pions, the phase space enhancement is such that points in agreement with standard cosmology (blue) can have an associated $\Delta r_K \sim \mathcal{O}(10^2)$.

Interesting information can also be drawn from analysing the correlated behaviour of these two observables, Δr_K and Δr_π . This is displayed in Fig. 9, which exhibits two interesting characteristics. The first one is that many points are grouped on the diagonal line, thus corresponding to a scenario where Δr_K and Δr_π are correlated. This is typically the case when sterile neutrinos are not kinematically accessible and the deviation is only due to the non-unitarity of \tilde{U}_{PMNS} , since the contribution from non-universality would be the same for both observables. Secondly, and concerning the size of the deviations, notice that Δr_K is always larger than Δr_π . This can be understood from the fact that for certain regimes, phase-space enhancements are possible for R_K and not for R_π . Such a result is particular to the ISS scenario. In models where the violation of lepton flavour universality is due to new charged Higgs interactions, one expects much larger deviations in K decays than in π decays (for example, in the case of supersymmetric models [93–98]).

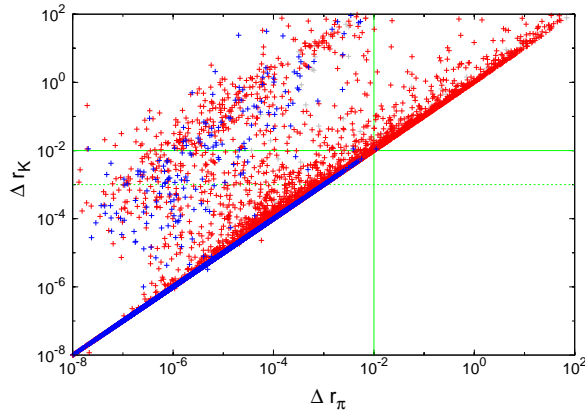


Figure 9: Δr_K versus Δr_π . Colour code as in Fig. 3. Full green lines denote the experimental upper bounds (for Δr_K a green dashed line denotes the expected future sensitivity).

Light meson decays - $R_{e,\mu}$ and $\Delta r_{e,\mu}$

In Fig. 10, we present the predictions regarding the observables $\Delta r_{e,\mu}$ introduced in Section 3.3. As can be seen from these figures, in the ISS scenario, especially in the regime of very light sterile neutrinos, one can indeed easily saturate the current experimental upper bound for Δr_e . However, saturating the experimental upper bound on Δr_μ is impossible in the regions of parameter space investigated in our analysis, except for some very specific points, which are mostly excluded by cosmological observations. For the heavy sterile regime (also corresponding to the cosmologically viable points), one in general recovers the SM limit.

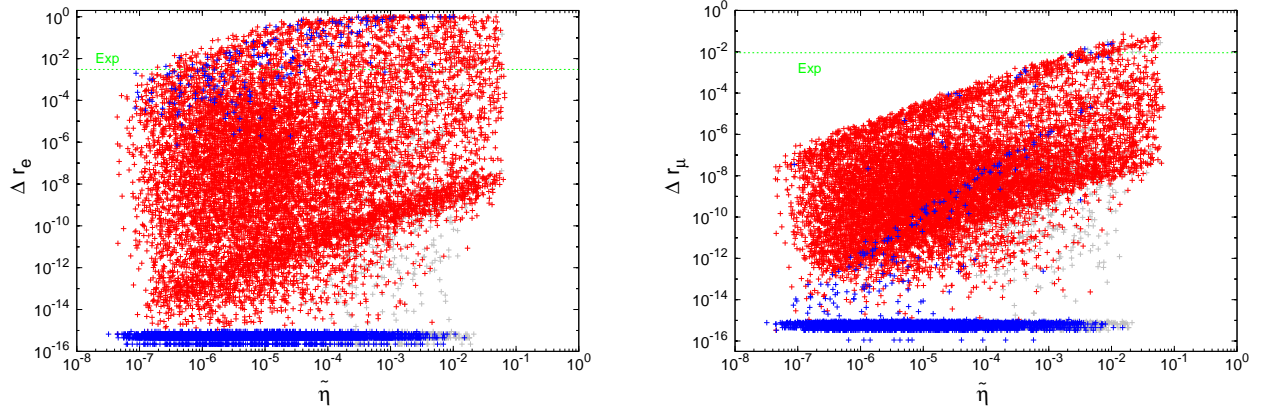


Figure 10: Ratios of leptonic light meson decay widths, Δr_e and Δr_μ , as a function of $\tilde{\eta}$. Colour code as in Fig. 3. Full green lines denote the experimental upper bounds.

Charmed meson decays - R_{D_s}

For completeness, we include in our analysis the predictions for R_{D_s} in the presence of sterile neutrinos⁹, displaying the results in Fig. 11. Current experimental measurements [24] are compatible with the SM prediction at the 1σ level, as is most of the parameter space here analysed. Interestingly, in this case the deviations from unitarity induced by the additional sterile states, increase the agreement between the ISS theoretical predictions and experimental observations.

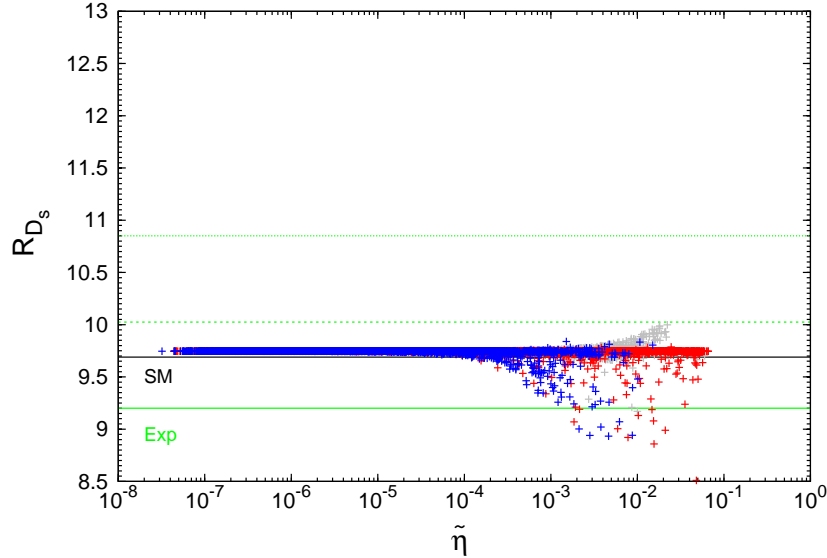


Figure 11: R_{D_s} as a function of $\tilde{\eta}$. Line and colour code as in Fig. 3.

⁹This observable, as well as the analogous ratio for D mesons, has been studied in Ref. [99]. Although we have a similar approach, our results differ from the ones obtained in that study, due to some discrepancies in the analytical formulae.

Charmed meson decays - $R_{D_s}^D$

We consider now the impact of the modified $W\ell\nu$ vertex for the ratio $R_{D_s}^D = \Gamma(D_s \rightarrow \tau\nu)/\Gamma(D \rightarrow \mu\nu)$. The results of our analysis, displayed as a function of $\tilde{\eta}$, are collected in Fig. 12. In this case we also consider the effect of a non-vanishing CP Dirac phase, δ . As seen from Fig. 12,

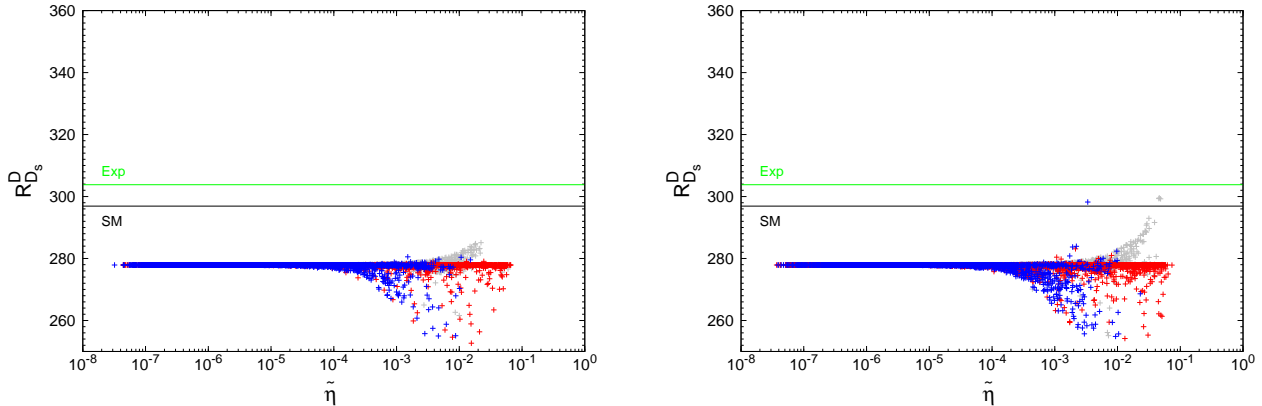


Figure 12: $R_{D_s}^D$ as a function of $\tilde{\eta}$. We also display the effect of the Dirac phase in the PMNS matrix: $\delta = 0$ (left) and randomly varied values, $\delta \in [0, 2\pi]$ (right). Line and colour code as in Fig. 3.

there is an offset between the SM expectation and our predictions in the limit $\tilde{\eta} \ll 1$ (where one recovers unitarity of the PMNS matrix). This is due to the fact that the hadronic parameters taken into our computation (see Eqs. (48, 49)) make use of new values for the ratio of f_{D_s} and f_D , determined from Lattice QCD [65], as well as the very precise experimental determination of f_K/f_π [67]. In view of this, we only present the central values for the experimental results. It is worth mentioning that taking other determinations of the ratio f_{D_s}/f_D , as for instance the one reported in [66], would translate into an overall (positive) correction of around 2%, which would have little impact on our phenomenological conclusions.

While for the previous observables a non-vanishing δ had a negligible impact, in the right panel of Fig. 12 one can see that for $\delta \neq 0$ a small number of points do succeed in alleviating the tension between theoretical predictions and experimental values - provided the above mentioned offset is indeed accounted for. A larger number of points would have indeed alleviated the tension, had they not been excluded by the recent MEG bound.

B meson decays - $\text{BR}(B \rightarrow \tau\nu)$

We have also considered the impact of the modified lepton charged current vertex regarding leptonic B decays. As mentioned in Section 3.3, this observable suffers from uncertainties associated with the determination of hadronic matrix elements (the B meson decay constant, f_B) and V_{CKM}^{ub} , as well as from experimental errors [73, 74]; in the absence of available data on $B \rightarrow (e, \mu)\nu$ decays, one cannot study a ratio of decay widths to test lepton flavour universality in B -meson decays. Our predictions¹⁰ (based on the input values for f_B and V_{CKM}^{ub} given in Section 3.3) for

¹⁰Notice that the present computation of $\text{BR}(B \rightarrow \tau\nu)$ corresponds to taking the central theoretical values for the different input parameters; due to the size of the theoretical error band, there is a significant overlap between

$\text{BR}(B \rightarrow \tau\nu)$ in the framework of the ISS, correspond to the SM theoretical prediction (within the % level). Thus, we do not display any plots for this observable.

4.6 $B^\pm \rightarrow D\ell\nu$ meson decays

We finally address the semileptonic decays of the charged B meson into a neutral D and a lepton pair, in particular the ratio $R(D)$, defined in Eq. (57). In view of the non-negligible contributions of the modified $W\ell\nu$ vertex (due to the presence of sterile neutrinos), we now investigate if the present framework could alleviate the existing tension between the SM prediction and the recent bounds (cf. Eqs. (58, 59)). In Fig. 13, we display $R(D)$ as a function of the non-unitarity parameter $\tilde{\eta}$ and, as done for $R_{D_s}^D$, we also illustrate the effect of a non-vanishing CP Dirac phase, δ .

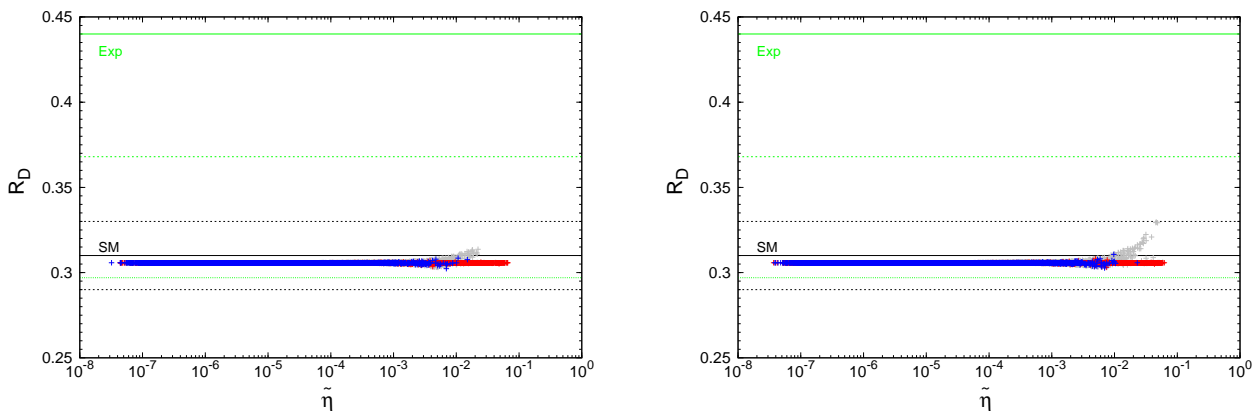


Figure 13: R_D as a function of $\tilde{\eta}$, displaying the effect of the Dirac phase in the PMNS matrix: $\delta = 0$ (left) and randomly varied values $\delta \in [0, 2\pi]$ (right). Line and colour code as in Fig. 3.

As one can see from Fig. 13, although the ISS could potentially give rise to contributions to $R(D)$ providing a minor alleviation of the existing tension between SM predictions and experimental measurements (especially in the case of non-vanishing CP Dirac phases), these are excluded due to the strong constraints arising from recent MEG bounds.

Other experimental measurements are expected in the future, and these will perhaps soften the deviation from the theoretical estimations¹¹. Moreover, observables related to semileptonic B decays are not free from QCD uncertainties (form factors), while such was not the case for other observables here studied. Finally, sources of NP in the lepton sector, other than the minimal inverse seesaw scenario studied here, can be considered.

5 Conclusions

In this work we have tried to reconcile theory and experiment in leptonic and semileptonic decays, under the hypothesis of New Physics contributions associated with the lepton sector. We have considered tree-level corrections to the SM charged current interaction $W\ell\nu$ vertex, due to the

¹¹the experimental and the theoretical 1σ intervals.

¹¹A huge effort is currently being made regarding the determination of B meson semileptonic decay form factors, as can be noticed from the FLAG review [66]. Very recent studies, after completion of our numerical analysis, have been reported [100], but the results do not change the conclusions of this work.

presence of sterile neutrinos (right-handed, or singlet components) which arise in several extensions of the SM aiming at addressing neutrino mass generation.

The phenomenological implications of these extensions are vast, and there are presently strong experimental and observational bounds (from laboratory, cosmology, as well as from electroweak precision tests) on the mass regimes and on the size of the active-sterile mixings.

In our analysis we have focused on the impact of the additional states for leptonic charged currents: the modification of the Standard Model $W\ell\nu$ vertex can lead to potentially large contributions to observables involving one or two neutrinos in the final state. We have derived complete analytical expressions for all the observables in the framework of the SM extended by sterile states, taking into account massive leptons and their mixings. In order to illustrate the impact of the sterile fermions, we have considered the framework of the inverse seesaw mechanism.

Although conducted for a specific seesaw realisation, our analysis reveals that New Physics in the lepton sector - in the form of additional sterile states - can indeed lead to contributions to some of the leptonic and semileptonic decays here considered (τ leptonic and mesonic decays, leptonic π , K , D , D_s decays and semileptonic $B \rightarrow D\ell\nu$ decays). Notice however that these are accompanied by sizable contributions to rare radiative lepton decays: in particular, new MEG bounds on $\text{BR}(\mu \rightarrow e\gamma)$ preclude important ISS contributions which would otherwise allow to alleviate the tension between theory and experiment. We extended our analysis to observables which are likely to be studied in the near future (for example $R_K^{\ell\tau}$), predicting their expected range for the investigated parameter space.

Our analysis reveals that, of the different investigated observables, $R_{K,\pi}$ are clearly the most powerful ones in constraining the model. Contrary to other observables, R_P is helicity suppressed in the SM, and as a consequence very small values are predicted. Any SM extension where helicity suppression is no longer present (or is at least alleviated) should then allow for sizable deviations in R_P , as is the case of the ISS scenario addressed in this work.

Acknowledgements

We are grateful to Damir Becirevic for many useful and enlightening discussions. A. V. thanks Tommaso Spadaro for his insight on the experimental perspectives of the NA62 experiment. This work has been partly done under the ANR project CPV-LFV-LHC NT09-508531. The work of C. W. is supported by the Spanish MINECO under grant FPA-2012-31880. The authors acknowledge partial support from the European Union FP7 ITN INVISIBLES (Marie Curie Actions, PITN-GA-2011-289442).

References

- [1] A. Kusenko, Phys. Rept. **481** (2009) 1 [arXiv:0906.2968 [hep-ph]].
- [2] K. N. Abazajian, M. A. Acero, S. K. Agarwalla, A. A. Aguilar-Arevalo, C. H. Albright, S. Antusch, C. A. Argüelles and A. B. Balantekin *et al.*, “Light Sterile Neutrinos: A White Paper,” arXiv:1204.5379 [hep-ph].
- [3] J. Schechter and J. W. F. Valle, Phys. Rev. D **22** (1980) 2227.
- [4] M. Gronau, C. N. Leung and J. L. Rosner, Phys. Rev. D **29** (1984) 2539.
- [5] R. E. Shrock, Phys. Lett. B **96** (1980) 159; R. E. Shrock, Phys. Rev. D **24** (1981) 1232.

- [6] E. Nardi, E. Roulet and D. Tommasini, *Phys. Lett. B* **327** (1994) 319 [hep-ph/9402224].
- [7] A. Abada, D. Das, A. M. Teixeira, A. Vicente and C. Weiland, *JHEP* **1302** (2013) 048 [arXiv:1211.3052 [hep-ph]].
- [8] A. Ilakovac and A. Pilaftsis, *Nucl. Phys. B* **437** (1995) 491 [hep-ph/9403398].
- [9] F. Deppisch and J. W. F. Valle, *Phys. Rev. D* **72** (2005) 036001 [hep-ph/0406040].
- [10] T. Asaka, S. Blanchet and M. Shaposhnikov, *Phys. Lett. B* **631** (2005) 151 [hep-ph/0503065].
- [11] A. Ibarra, E. Molinaro and S. T. Petcov, *JHEP* **1009** (2010) 108 [arXiv:1007.2378 [hep-ph]].
- [12] R. N. Mohapatra and J. W. F. Valle, *Phys. Rev. D* **34** (1986) 1642.
- [13] P. Minkowski, *Phys. Lett. B* **67** (1977) 421.
- [14] T. Yanagida, in *KEK lectures*, ed. O. Sawada and A. Sugamoto, KEK, 1979; M Gell-Mann, P Ramond, R. Slansky, in *Supergravity*, ed. P. van Nieuwenhuizen and D. Freedman (North Holland, 1979).
- [15] R. N. Mohapatra and G. Senjanovic, *Phys. Rev. Lett.* **44** (1980) 912.
- [16] D. V. Forero, M. Tortola and J. W. F. Valle, *Phys. Rev. D* **86** (2012) 073012 [arXiv:1205.4018 [hep-ph]].
- [17] G. L. Fogli, E. Lisi, A. Marrone, D. Montanino, A. Palazzo and A. M. Rotunno, *Phys. Rev. D* **86** (2012) 013012 [arXiv:1205.5254 [hep-ph]].
- [18] M. C. Gonzalez-Garcia, M. Maltoni, J. Salvado and T. Schwetz, *JHEP* **1212** (2012) 123 [arXiv:1209.3023 [hep-ph]].
- [19] X. Qian, C. Zhang, M. Diwan and P. Vogel, arXiv:1308.5700 [hep-ex].
- [20] S. Antusch, J. P. Baumann and E. Fernandez-Martinez, *Nucl. Phys. B* **810** (2009) 369 [arXiv:0807.1003 [hep-ph]].
- [21] F. del Aguila, J. de Blas and M. Perez-Victoria, *Phys. Rev. D* **78** (2008) 013010 [arXiv:0803.4008 [hep-ph]].
- [22] E. Akhmedov, A. Kartavtsev, M. Lindner, L. Michaels and J. Smirnov, *JHEP* **1305** (2013) 081 [arXiv:1302.1872 [hep-ph]].
- [23] L. Basso, O. Fischer and J. J. van der Bij, “Precision tests of unitarity in leptonic mixing,” arXiv:1310.2057 [hep-ph].
- [24] J. Beringer *et al.* [Particle Data Group Collaboration], *Phys. Rev. D* **86** (2012) 010001.
- [25] A. Atre *et al.*, *JHEP* **0905** (2009) 030 [arXiv:0901.3589 [hep-ph]].
- [26] L. Lello and D. Boyanovsky, *Phys. Rev. D* **87** (2013) 073017 [arXiv:1208.5559 [hep-ph]].
- [27] J. Adam *et al.* [MEG Collaboration], “New constraint on the existence of the $\mu^+ \rightarrow e^+ \gamma$ decay,” arXiv:1303.0754 [hep-ex].

- [28] A. Ilakovac and A. Pilaftsis, Phys. Rev. D **80** (2009) 091902 [arXiv:0904.2381 [hep-ph]].
- [29] R. Alonso, M. Dhen, M. B. Gavela and T. Hambye, JHEP **1301** (2013) 118 [arXiv:1209.2679 [hep-ph]].
- [30] D. N. Dinh, A. Ibarra, E. Molinaro and S. T. Petcov, JHEP **1208** (2012) 125 [arXiv:1205.4671 [hep-ph]].
- [31] A. Ilakovac, A. Pilaftsis and L. Popov, Phys. Rev. D **87** (2013) 053014 [arXiv:1212.5939 [hep-ph]].
- [32] A. Abada, D. Das, A. Vicente and C. Weiland, JHEP **1209** (2012) 015 [arXiv:1206.6497 [hep-ph]].
- [33] P. S. Bhupal Dev, R. Franceschini and R. N. Mohapatra, Phys. Rev. D **86** (2012) 093010 [arXiv:1207.2756 [hep-ph]].
- [34] C. G. Cely, A. Ibarra, E. Molinaro and S. T. Petcov, Phys. Lett. B **718** (2013) 957 [arXiv:1208.3654 [hep-ph]].
- [35] P. Bandyopadhyay, E. J. Chun, H. Okada and J. -C. Park, JHEP **1301** (2013) 079 [arXiv:1209.4803 [hep-ph]].
- [36] F. F. Deppisch, M. Hirsch and H. Pas, J. Phys. G **39** (2012) 124007 [arXiv:1208.0727 [hep-ph]].
- [37] M. Agostini *et al.* [GERDA Collaboration], Phys. Rev. Lett. **111** (2013) 122503 [arXiv:1307.4720 [nucl-ex]].
- [38] J. C. Helo, M. Hirsch, S. G. Kovalenko and H. Pas, Phys. Rev. D **88** (2013) 011901 [arXiv:1303.0899 [hep-ph]].
- [39] J. C. Helo, M. Hirsch, H. Ps and S. G. Kovalenko, Phys. Rev. D **88** (2013) 073011 [arXiv:1307.4849 [hep-ph]].
- [40] S. Chatrchyan *et al.* [CMS Collaboration], Phys. Lett. B **717** (2012) 109 [arXiv:1207.6079 [hep-ex]].
- [41] A. Y. Smirnov and R. Zukanovich Funchal, Phys. Rev. D **74** (2006) 013001 [hep-ph/0603009].
- [42] G. Gelmini *et al.*, JCAP **0810** (2008) 029 [arXiv:0803.2735 [astro-ph]].
- [43] B. Dasgupta and J. Kopp, “A ménage à trois of eV-scale sterile neutrinos, cosmology, and structure formation,” arXiv:1310.6337 [hep-ph].
- [44] D. Gorbunov and M. Shaposhnikov, JHEP **0710** (2007) 015 [arXiv:0705.1729 [hep-ph]].
- [45] B. A. Kniehl, F. Madricardo and M. Steinhauser, Phys. Rev. D **62** (2000) 073010 [hep-ph/0005060].
- [46] J. Alcaraz *et al.* [ALEPH and DELPHI and L3 and OPAL and LEP Electroweak Working Group Collaborations], “A Combination of preliminary electroweak measurements and constraints on the standard model,” hep-ex/0612034.

- [47] A. Filipuzzi, J. Portoles and M. Gonzalez-Alonso, Phys. Rev. D **85** (2012) 116010 [arXiv:1203.2092 [hep-ph]].
- [48] A. Pich, I. Boyko, D. Dedovich and I. I. Bigi, Int. J. Mod. Phys. A **24S1** (2009) 715.
- [49] B. Aubert *et al.* [BaBar Collaboration], Phys. Rev. Lett. **105** (2010) 051602 [arXiv:0912.0242 [hep-ex]].
- [50] A. Anastassov *et al.* [CLEO Collaboration], Phys. Rev. D **55** (1997) 2559 [Erratum-ibid. D **58** (1998) 119904].
- [51] A. Ferroglia, C. Greub, A. Sirlin and Z. Zhang, Phys. Rev. D **88** (2013) 033012 [arXiv:1307.6900 [hep-ph]].
- [52] M. Fael, L. Mercolli and M. Passera, “W-propagator corrections to muon and tau leptonic decays,” arXiv:1310.1081 [hep-ph].
- [53] V. Cirigliano and I. Rosell, Phys. Rev. Lett. **99** (2007) 231801 [arXiv:0707.3439 [hep-ph]].
- [54] M. Finkemeier, Phys. Lett. B **387** (1996) 391 [hep-ph/9505434].
- [55] E. Goudzovski [NA48/2 and NA62 Collaboration], PoS EPS **HEP2011** (2011) 181 [arXiv:1111.2818 [hep-ex]].
- [56] C. Lazzeroni *et al.* [NA62 Collaboration], Phys. Lett. B **719** (2013) 326 [arXiv:1212.4012 [hep-ex]].
- [57] G. Czapek *et al.*, Phys. Rev. Lett. **70** (1993) 17.
- [58] E. Goudzovski [NA48/2 and NA62 Collaborations], arXiv:1208.2885 [hep-ex].
- [59] Steffen Strauch [for the TREK Collaboration], ”Searches for New Physics with the TREK Detector”, PoS(KAON13)014, http://pos.sissa.it/archive/conferences/181/014/KAON13_014.pdf
- [60] D. Pocanic *et al.*, arXiv:1210.5025 [hep-ex].
- [61] C. Malbrunot *et al.*, AIP Conf. Proc. **1441** (2012) 564.
- [62] T. Spadaro, private communication.
- [63] H. -B. Li, Int. J. Mod. Phys. Conf. Ser. **02** (2011).
- [64] P. Naik *et al.* [CLEO Collaboration], Phys. Rev. D **80** (2009) 112004 [arXiv:0910.3602 [hep-ex]].
- [65] D. Becirevic, B. Blossier, A. Gerardin, A. Le Yaouanc and F. Sanfilippo, Nucl. Phys. B **872** (2013) 313 [arXiv:1301.7336 [hep-ph]].
- [66] S. Aoki, Y. Aoki, C. Bernard, T. Blum, G. Colangelo, M. Della Morte, S. Drr and A. X. E. Khadra *et al.*, arXiv:1310.8555 [hep-lat].
- [67] M. Antonelli, D. M. Asner, D. A. Bauer, T. G. Becher, M. Beneke, A. J. Bevan, M. Blanke and C. Bloise *et al.*, Phys. Rept. **494** (2010) 197 [arXiv:0907.5386 [hep-ph]].

- [68] J. Charles, O. Deschamps, S. Descotes-Genon, R. Itoh, H. Lacker, A. Menzel, S. Monteil and V. Niess *et al.*, Phys. Rev. D **84** (2011) 033005 [arXiv:1106.4041 [hep-ph]].
- [69] M. Bona *et al.* [UTfit Collaboration], Phys. Lett. B **687** (2010) 61 [arXiv:0908.3470 [hep-ph]].
- [70] R. J. Dowdall *et al.* [HPQCD Collaboration], Phys. Rev. Lett. **110** (2013) 222003 [arXiv:1302.2644 [hep-lat]].
- [71] A. Bazavov *et al.* [Fermilab Lattice and MILC Collaborations], Phys. Rev. D **85** (2012) 114506 [arXiv:1112.3051 [hep-lat]].
- [72] B. Blossier, Phys. Rev. D **84** (2011) 097501 [arXiv:1106.2132 [hep-lat]].
- [73] I. Adachi *et al.* [Belle Collaboration], Phys. Rev. Lett. **110** (2013) 131801 [arXiv:1208.4678 [hep-ex]].
- [74] B. Aubert *et al.* [BaBar Collaboration], Phys. Rev. D **77** (2008) 011107 [arXiv:0708.2260 [hep-ex]].
- [75] J. P. Lees *et al.* [BaBar Collaboration], Phys. Rev. Lett. **109** (2012) 101802 [arXiv:1205.5442 [hep-ex]].
- [76] D. Becirevic, N. Kosnik and A. Tayduganov, Phys. Lett. B **716** (2012) 208 [arXiv:1206.4977 [hep-ph]].
- [77] S. Fajfer, J. F. Kamenik and I. Nisandzic, Phys. Rev. D **85** (2012) 094025 [arXiv:1203.2654 [hep-ph]].
- [78] V. G. Luth, “Proceedings of 10th Conference on Flavor Physics and CP Violation (FPCP 2012): Hefei, Anhui, China, May 21-25, 2012”, eds. Z. -G. Zhao, J. -X. Lu and Q. Wang, SLAC-eConf-C120521 [arXiv:1209.4674 [hep-ex]].
- [79] A. Celis, M. Jung, X. -Q. Li and A. Pich, JHEP **1301** (2013) 054 [arXiv:1210.8443 [hep-ph]].
- [80] C. Schwanda, talk at “Portoroz 2013: Probing the Standard Model and New Physics at Low and High Energies”.
- [81] J. P. Lees *et al.* [BaBar Collaboration], “Measurement of an Excess of $B \rightarrow D^{(*)}\tau\nu$ Decays and Implications for Charged Higgs Bosons,” arXiv:1303.0571 [hep-ex].
- [82] B. Aubert *et al.* [BaBar Collaboration], Phys. Rev. Lett. **104** (2010) 011802 [arXiv:0904.4063 [hep-ex]].
- [83] J. A. Bailey, A. Bazavov, C. Bernard, C. M. Bouchard, C. DeTar, D. Du, A. X. El-Khadra and J. Foley *et al.*, Phys. Rev. D **85** (2012) 114502 [Erratum-ibid. D **86** (2012) 039904] [arXiv:1202.6346 [hep-lat]].
- [84] G. M. de Divitiis, E. Molinaro, R. Petronzio and N. Tantalo, Phys. Lett. B **655** (2007) 45 [arXiv:0707.0582 [hep-lat]].
- [85] S. Faller, A. Khodjamirian, C. Klein and T. Mannel, Eur. Phys. J. C **60** (2009) 603 [arXiv:0809.0222 [hep-ph]].
- [86] K. Azizi, Nucl. Phys. B **801** (2008) 70 [arXiv:0805.2802 [hep-ph]].

- [87] M. C. Gonzalez-Garcia and J. W. F. Valle, Phys. Lett. B **216** (1989) 360.
- [88] J. A. Casas and A. Ibarra, Nucl. Phys. B **618** (2001) 171 [hep-ph/0103065].
- [89] D. V. Forero *et al.*, JHEP **1109** (2011) 142 [arXiv:1107.6009 [hep-ph]].
- [90] M. Malinsky, T. Ohlsson and H. Zhang, Phys. Rev. D **79** (2009) 073009 [arXiv:0903.1961 [hep-ph]].
- [91] P. S. B. Dev and R. N. Mohapatra, Phys. Rev. D **81** (2010) 013001 [arXiv:0910.3924 [hep-ph]].
- [92] V. Cirigliano, S. Gardner and B. Holstein, Prog. Part. Nucl. Phys. **71** (2013) 93 [arXiv:1303.6953 [hep-ph]].
- [93] A. Masiero, P. Paradisi and R. Petronzio, Phys. Rev. D **74** (2006) 011701 [hep-ph/0511289].
- [94] M. J. Ramsey-Musolf, S. Su and S. Tulin, Phys. Rev. D **76** (2007) 095017 [arXiv:0705.0028 [hep-ph]].
- [95] A. Masiero, P. Paradisi and R. Petronzio, JHEP **0811** (2008) 042 [arXiv:0807.4721 [hep-ph]].
- [96] J. Ellis, S. Lola and M. Raidal, Nucl. Phys. B **812** (2009) 128 [arXiv:0809.5211 [hep-ph]].
- [97] J. Gierbach and U. Nierste, “ $\Gamma(K \rightarrow e\nu)/\Gamma(K \rightarrow \mu\nu)$ in the Minimal Supersymmetric Standard Model,” arXiv:1202.4906 [hep-ph].
- [98] R. M. Fonseca, J. C. Romao and A. M. Teixeira, Eur. Phys. J. C **72** (2012) 2228 [arXiv:1205.1411 [hep-ph]].
- [99] B. Wang, M. -G. Zhao, K. -S. Sun and X. -Q. Li, Chin. Phys. C **37** (2013) 7, 073101 doi:10.1088/1674-1137/37/7/073101.
- [100] M. Atoui, B. Blossier, V. Morénas, O. Pène and K. Petrov, “Semileptonic $B \rightarrow D^{**}$ decays in Lattice QCD: a feasibility study and first results,” arXiv:1312.2914 [hep-lat].